International Journal of General Medicine

Dovepress
open access to scientific and medical research

Open Access Full Text Article

ORIGINAL RESEARCH

Validation of Jianpi Qingre Tongluo Recipe in Reducing Inflammation and Dyslipidemia in Osteoarthritis via Lnc RNA HOTAIR/APN/PI3K/AKT

Xiaolu Chen[1–3], Jian Liu[1,2], Guizhen Wang[1,2], Yanqiu Sun[1,2], Xiang Ding[1–3], Xianheng Zhang[1–3]

[1]Department of Rheumatology and Immunology, First Affiliated Hospital of Anhui University of Traditional Chinese Medicine, Hefei, Anhui Province, 230038, People's Republic of China; [2]Institute of Rheumatology, Anhui University of Chinese Medicine, Hefei, Anhui Province, 230012, People's Republic of China; [3]Anhui University of Traditional Chinese Medicine, Hefei, People's Republic of China

Correspondence: Jian Liu, Department of Rheumatology and Immunology, First Affiliated Hospital of Anhui University of Traditional Chinese Medicine, Hefei, Anhui Province, 230038, People's Republic of China, Tel +86 551 62838582, Fax +86 551 62821605, Email liujianahzy@126.com

Objective: Jianpi Qingre Tongluo Recipe (JQP) has been widely used in clinical practice, and its anti-Osteoarthritis (OA) effectiveness and specific mechanism have been concerned. This study aims to explore the clinical effect of JQP in reducing inflammation and dyslipidemia in OA and the molecular mechanism.

Methods: The clinical efficacy of JQP in OA treatment was assessed through data mining. Through the network pharmacology technology, the interactive network of "active component-target-disease" was developed, the interaction relationship of the related proteins was analyzed, and enrichment analysis of gene pathway biological process was conducted. Molecular docking was carried out with PyMOL and AutodockTools-1.5.7. Finally, cell experiments were used to verify JQP's delay of immune inflammation in OA.

Results: We found that JQP could ameliorate the immune inflammatory and lipid metabolism indicators; reduce VAS and SAS score in OA. A total of 98 genes overlapped between target genes of JQP and OA. TNF, IL-6, IL-1β, and AKT1 shared the highest centrality among all target genes. KEGG analysis unveiled that 98 intersection genes were predominantly enriched in PI3K/AKT pathway in the anti-OA system. In vitro, after peripheral blood mononuclear cell (PBMC) stimulation, inflammatory cytokines imbalances and the expressions of adiponectin (APN) were decreased in osteoarthritis-chondrocytes (OA-CH). Furthermore, JQP-containing serum protected OA-CHs through down-regulating HOTAIR levels, thereby up-regulating APN and depressing PI3K/AKT pathway.

Conclusion: This study suggests that JQP might reduce inflammation and improve lipid metabolism of OA by regulating HOTAIR/APN/PI3K/AKT. Our results bring a new solution for OA.

Keywords: osteoarthritis, chondrocytes, inflammation, LncRNA HOTAIR/APN/PI3K/AKT

Introduction

As a frequently occurring chronic diseases, osteoarthritis (OA) possesses complex and multifactorial epidemiology and manifests as pain, stiffness, and reduced mobility resulting from the breakdown of joint cartilage.[1] It is a holistic joint disease involving all joint tissues (synovial membrane, menisci, subchondral bone, cartilage and infrapatellar fat pad).[2] Inflammation is the most pivotal factor initiating and amplifying OA.[3] Inflammatory cytokines are produced during cellular inflammation. Notably, synovial membrane and infrapatellar fat pad are the OA tissues inflamed and fibrotic, involved in OA pain and producing cytokines impacting on other tissues,[4] previous in vivo and in vitro experiments have proved that inflammatory cytokines participate in the occurrence and development of OA, can induce the phosphorylation of AKT, produce chondrocyte (CHs) inflammation, and accelerate the degradation of cartilage tissues and cells.[5,6] In addition, abnormally lowers high-density lipoprotein cholesterol (HDL-C) and apolipoprotein A1 (apo-A1) levels, giving rise to inflammation and OA deterioration.[7] Studies have shown that body fat is negatively correlated with adiponectin (APN),[8,9] indicating that APN is a protective factor for abnormal lipid metabolism. Peripheral blood mononuclear cells (PBMCs) can elevate inflammatory cytokine expression[10–12] and boost the release of metalloproteinases from CHs and induce cartilage destruction.[13] Prior

Received: 9 May 2024
Accepted: 20 July 2024
Published: 26 July 2024

studies[14,15] have reported that PBMCs exhibit up-regulation of interleukin (IL)-6 and tumor necrosis factor alpha (TNF-α), and down-regulation of IL-10 and APN. Additionally, the APN/adipoR1 axis promotes anti-inflammatory factor secretion and inhibits pro-inflammatory factor release from PBMCs. Therefore, PBMCs co-culture with CHs can damage CHs and induce inflammatory environment, while APN acts as a cartilage protective factor and regulates inflammation.

No effective drugs have been found to treat OA in the early stage. Although corticosteroids, hyaluronan, and non-steroidal anti-inflammatory drugs have been clinically used to treat OA,[16] they fail to reverse cartilage injury and halt the significant progression of OA to the stage of requiring prosthetic replacement.[17] Therefore, in order to better treat and postpone the progression of OA, there is an urgent need for new therapies that can limit cartilage destruction. Natural herbal compounds are thought to be promising therapeutic agents for immunological illnesses that could stop the disease's progression and have fewer adverse effects. As a result, more researchers are now interested in these compounds.[18,19]

Long non-coding RNAs (lncRNAs) participant in numerous physiological and pathological processes, like OA.[20] As a trans-acting lncRNA, HOTAIR possesses a function of modulating transcription. HOTAIR has been shown to exist in cancer as a novel oncogenic propellant, is a potential prognostic factor and therapeutic target for human cancer.[21,22] In addition, studies have summarized the function of HOTAIR in regulating protein degradation, proinflammatory, immune signaling and DNA damage response,[23] which proves that it is in the important position of immune inflammatory response. Former research[24,25] have unraveled greatly higher HOTAIR expression in OA-CHs than in normal CHs and the promoting effect of small interfering RNA (si)-HOTAIR on OA-CH proliferation. HOTAIR is a critical lncRNA up-regulated in OA and affecting OA progression, research on HOTAIR may help to clarify biomarkers or therapeutic targets for OA. PI3K/AKT pathway, a classic inflammatory pathway, is closely related to inflammatory signals.[26] When it is activated, inflammatory signals like IL-1β, TNF-α, and IL-6 are released, which worsen the course of OA.[27] Furthermore, we have discovered that the pathophysiology of OA is concurrently mediated by HOTAIR overexpression and PI3K/AKT pathway activation.[28]

Over the past 30 years, JQP are often widely used in combination with the treatment of OA with amazing curative results.[29,30] JQP consists of two capsules: Huangqin chubi capsule (HQC; Patent no. ZL201110095718.X; Anhui medical system drug approval No. Z20200001) and Xinfeng capsule (XFC; Patent no. ZL201310011369.8; Anhui medical system drug approval No. Z20050062), made up of the following eight traditional Chinese medicines:[31–33] *Scutellaria baicalensis* Georgi (http://mpns.kew.org), *Gardenia jasminoides* J.Ellis (http://mpns.kew.org), *Clematis chinensis* Osbeck (http://mpns.kew.org), *Juglans regia* L. (http://mpns.kew.org), *Astragalus mongholicus* Bunge (http://mpns.kew.org), *Coix lacryma-jobi* L. (http://mpns.kew.org), *Tripterygium wilfordi*i Hook. f. (http://mpns.kew.org), and *Scolopendra subspinipes mutilans* L. Koch (https://db.ouryao.com), combined in a ratio of 10:9:10:5:20:20:10:1. JQP follows rigorous quality standards confirmed by UPLC-MS/MS technology and high performance liquid chromatography (HPLC) fingerprinting.[34,35] The core ingredients that have been confirmed and recommended are baicalin, amygdalin, puerarin, daidzin, luteolin, salvianolic acid B, geniposide, danshensu, coixol, protocatechuic aldehyde, and daidzein.

We have previously discovered that JQP-containing serum dramatically lowered IL-1β, TNF-α, and IL-6 expression, while markedly augmented IL-4 and IL-10 expression.[36,37] In particular, JQP has the advantages of high safety and few side effects in the treatment of OA, so it has been increasingly used by experienced clinicians to treat OA.[30,38] However, the effect of JQP on OA disease progression, CH inflammation and injury are unknown and few studies have been reported. Therefore, this study recruited OA patients for clinical trials to explore the efficacy observation of JQP in the treatment of OA, and further designed in vitro cell experiments to explore the protective effect of JQP on OA and clarify its underlying mechanisms by preparing pharmaceutical serum containing JQP (Supplementary Picture 1).

Materials and Methods

Clinical Research

Participants and Samples

Between November 2022 and May 2023, we recruited age- and sex-matched OA patients and healthy control (HC) participants from the First Affiliated Hospital of Anhui University of Traditional Chinese Medicine. Inclusion criteria: All OA participants met the 2019 Guidelines for the Diagnosis of OA;[39] All HC participants were gender - and age-

matched healthy volunteers. Exclusion criteria: were on pregnancy; serious mental illness; serious infectious disease or serious cardiovascular and cerebrovascular disease; were on immunosuppressants. Both HC group and JQP group were observed for 1 month. All subjects in JQP group were asked to take JQP (XFC, 3 capsules/time, 3 times/day; HQC, 3 capsules/time, 3 times/day). The current research was ratified by the Ethical Committee of Scientific Research in the First Affiliated Hospital of Anhui University of Traditional Chinese Medicine (2023AH-52) and conformed to pertinent Declaration of Helsinki rules,[40] with informed consent obtained from all participants.

Blood samples from all participants were taken for detecting of laboratory indicators, and in addition, Venous blood (5 mL) was drawn from both OA patients and healthy individuals and diluted with normal saline of equal volume. The prepared samples were slowly mixed with lymphocyte separation solutions of equal volume, and they were centrifuged for 20 minutes at 2000 revolutions per minute. The centrifuge tube with the white flocculent (PBMCs) was moved to the one that was clean. The tube was filled with the same volume of regular saline and mixed. An 8-min centrifugation at 800 rpm and two washings were then performed. The samples were blown, then placed in a culture flask and allowed to incubate before being used.

Detecting of Laboratory Indicators

Erythrocyte sedimentation rate (ESR, reference value: male 0–15mm/h, female 0–20 mm/h) was measured by radio-immunoassay. Hyper-sensitivity C-reactive protein (hs-CRP, reference value: 0–1mg/L), complement C3/4 (C3/4, reference value: 0.8–0.1.5 g/L; 0.2–0.0.6 g/L), immunoglobulin A/G/M (IgA/G/M, reference value: 0.7–3.5 g/L; 7.0–16.6 g/L; 0.5–2.6 g/L), Total cholesterol (TC, reference value: ≦5.2 mmol/L) and Triglyceride (TG, reference value: ≦1.7 mmol/L) were measured by colorimetry and were strictly operated by clinical staff of Anhui Provincial Hospital of Traditional Chinese Medicine in accordance with regulations.

Scale Score Method

All OA patients completed paper versions of Self Rating Anxiety Scale (SAS), Self Rating Depression Scale (SDS), and visual analogue scale (VAS) under the guidance of two professional physicians. One doctor was plugged into the data processing system, while the other oversaw quality control.

On the VAS, 0 represented no pain, 1–3 represented mild pain, 4–6 represented moderate pain, and 7–10 represented severe pain. Anxiety is classified as none at an SAS score of 50 or below, mild anxiety at 50–59, moderate anxiety at 60–69, and severe anxiety at 70 or more. A score of less than 50 on the SDS indicates no depression, a score between 50 and 59 denotes mild depression, and a score between 60 and 69 denotes moderate to severe depression. Severe depression is thought to be indicated by a score greater than 70.[41]

Association Rule Mining (ARM)

The rise and decline of clinical indexes were set to "T" and "F", respectively. The association between JQP and clinical observation indexes was determined with the Apriori module in SPSS Clementine 11.1 software. The formulae were as follows:[42]

$$\text{Support}(X \rightarrow Y) = \sigma\frac{(X \cup Y)}{N}$$

$$\text{Confidence}(X \rightarrow Y) = \sigma\frac{(X \cup Y)}{\sigma(X)}$$

$$\text{Lift}(X \rightarrow Y) = \text{Confidence}\frac{(X \rightarrow Y)}{\sigma(Y)}$$

Random Walking Applicable Formula

Using the random walking model, the Oracle Developer Suite 10 g was adopted to test the relationship between JQP and important covariates. The formula was as follows:[30,43]

$$y(l) = \sum_{i=1}^{l} u(i)$$

$$F^2(l) = \overline{\left[\Delta y(l) - \overline{\Delta y(l)}\right]^2} = \overline{[\Delta y(l)]^2} - \left[\overline{\Delta y(l)}\right]^2$$

$$\Delta y(l) = y(l_0 + l_1) - y(l_0)$$

$$F^2(l) \sim l^{\alpha}, \text{with } \alpha \neq \frac{1}{2}$$

Network Pharmacology and Molecular Docking

Screening of JQP Components and Targets

JQP was prepared from eight kinds of herbs, namely, Scutellaria baicalensis Georgi, Gardenia jasminoides J.Ellis, Clematis chinensis Osbeck, Juglans regia L., Astragalus mongholicus Bunge, Coix lacryma-jobi L., Tripterygium wilfordii Hook. f., and Scolopendra subspinipes mutilans L.Koch. The active ingredients of these herbs were determined by inputting them into the Traditional Chinese Medicine Systems Pharmacology Database and Analysis Platform (TCMSP) and screened through absorption, distribution, metabolism, and excretion (ADME), with the criteria of oral bioavailability (OB) ≥30% and drug-likeness (DL) ≥0.18. With the Herb database, the targets of active ingredients in JQP were supplemented.

Potential Target Identification and Construction of a Compound-Target Network

First, active ingredient and target information for JQP was gathered as described earlier. Then, OA-related targets were retrieved in the Therapeutic Target Database (TTD), DrugBank database, Online Mendelian Inheritance in Man (OMIM), and Genecards database, with "osteoarthritis" as the keyword. Drug- and disease-related targets were standardized with the UniProt database. Next, a Venn diagram was employed to intersect the standardized drug-related targets with the disease-related targets. After the intersected targets and active ingredients were uploaded to Cytoscape 3.8.2, the merging functionality in Cytoscape was applied to build the compound-target network.

Protein-Protein Interaction (PPI) Network Construction and Core Target Screening

The PPI network and data file were obtained by introducing the therapeutic targets of JQP and OA-related targets to STRING (https://string-db.org), followed by the importing of the PPI data in to Cytoscape 3.8.2 and PPI network analysis with the "MCODE" plugin.

Gene Ontology (GO) Functional Enrichment and Kyoto Encyclopedia of Genes and Genomes (KEGG) Pathway Enrichment Analyses

Metascape was adopted for GO and KEGG analyses. GO functions and KEGG pathways were sorted by count. The top 20% GO terms [cellular component (CC), biological process (BP), and molecular function (MF)] and KEGG pathways with the highest enrichment were selected for further analysis.

Potential Active Ingredient and Protein Molecular Docking for JQP

PubChem (https://pubchem.ncbi.nlm.nih.gov/) was employed for retrieving the 2D structure of the potential ingredients, followed by the minimization of the energy of small molecules with ChemBio3D 2014 software. Subsequent to the conversion of the 2D structure to the 3D structure, the 3D structure of the core target protein was attained from the Protein Data Bank database (http://www.rcsb.org). Target protein receptor molecules were processed with Pymol software, such as dehydration and removal of ligand small molecules, and hydrogenated with Autodock Tools 4.2.6 software. The center coordinate and size of the box were set as per the location of the active site of the protein molecule and its potential region of action on the ligand small molecule. AutoDock Vina was adopted for molecular docking, with lower binding energy representing higher affinity between the receptor and ligand. Binding energies ≤0 kcal/mol denoted that ingredients could bind to and interact with targets, whilst binding energies < −5 kcal/mol were indicative of extremely

strong binding. The results of docking with optimal binding between each core target protein and active ingredient are simultaneously displayed in 2D images and 3D structures.

Administration Method of JQP and Preparation of JQP-Medicated Serum

The JQP needed for the experiment came from the pharmacy center of the First Affiliated Hospital of Anhui University of Chinese Medicine. Twenty Specific pathogen Free (SPF) male Sprague-Dawley (SD) rats (aged 6–8 weeks, weighing 180 ± 20 g, license number: SCXK (Liao) 2020–0001), purchased from Suzhou Xishan Biotechnology Co., LTD. (Suzhou, China). The rats were fed in cells with a temperature of 20–24°C and humidity of 40–60%. All the rats had free access to food and water.

After one week of adaptive feeding, 20 male SD rats (SPF grade) were randomly allocated into blank control and JQP groups (10 rats/group). Rats in the JQP group were given JQP (2.592 g/kg; volume: 10 mL/kg) by gavage. Rats in the control group were administered normal saline. All the rats were treated for 7 days. Subsequent to anesthesia, blood was drawn from the abdominal aorta of rats, centrifuged, filtered, and water-bathed at 56°C for 30 min for complement inactivation. In addition, a filter membrane with a diameter of 0.2 μm is used for sterilization. Finally, we obtained serum from normal rats and serum containing JQP. For the JQP group, JQP-containing serum was added to the OA-CH culture medium at 20% of the final medium concentration.[32] For the control group, the equivalent volume of cell medium without drug-containing serum was added. Approved by Animal Ethics Committee of Anhui University of Chinese Medicine (AHUCM-rats-2023,020).

Cell Experiment

Co-Culture of PBMCs with CHs from OA Patients and Transfection

Human primary OA chondrocytes (OA-CH), NO. JDBG200751, purchased from Sebkon (Shanghai) Biotechnology Co., LTD. PBMCs were extracted and placed into Transwell chambers (96-well plate, NEST, 701001), followed by the supplementation of Dulbecco's Modified Eagle Medium (DMEM, Hyclone, SH30022.01; 75 μL). Following digestion (Pancreatic enzyme, Beyotime, C0205), CHs were centrifuged. Following the media's disposal (FBS, BI, 04-001-1ACS), CHs were seeded into the lower chamber and resuspended with medium, followed by two phosphate buffer saline washes. Afterward, 100 μL of DMEM was then added. Different amounts of OA-PBMCs were introduced to the upper chamber after cell adhesion. Lastly, CCK-8 was used to screen for the best stimulation concentration for PBMCs. CHs underwent co-culture with DMEM encompassing 100 U/mL penicillin and 0.1 mg/mL streptomycin under the conditions of 5% CO_2 and 37°C until 70–90% CH confluence. With Lipofectamine 2000, OA-PBMCs + OA-CH (PC) was transfected with pcDNA3.1-LncRNA HOTAIR or si-LncRNA HOTAIR plasmids or corresponding NC plasmids (all plasmids from GenePharma, Shanghai, China) and incubated for 24 h. Below are the primer sequences: siRNA (si)-NC (forward primer: 5'-UUCUCCGAACGUGUCACGUTT-3', reverse primer: 5'-ACGUGACACGUUCGGAGAATT-3'); si-HOTAIR-1# (forward primer: 5'-GAUGUUUACAAGACCAGAAAU -3', reverse primer: 5'-UUCUGGUCUUGUAAACAUCAG-3'), si-HOTAIR-2# (forward primer: 5'-AGACGAAGGUGAAAGCGAACC-3', reverse primer: 5'-UUCGCUUUCACCUUCGUCUGG-3'); si-HOTAIR-3# (forward primer: 5'-GCUUCGCAGUGGAAUGGAACG-3', reverse primer: 5'-UUCCAUUCCACUGCGAAGCGG-3').

Reverse Transcription-Quantitative Polymerase Chain Reaction (RT-qPCR)

Trizol was used to collect total OA-CHs or PCs RNA, which was then subjected to an amplification and reverse transcription procedure. Reverse transcription was performed using the PrimeScript™RT reagent Kit with gDNA Eraser (TaKaRa, RR047A). mRNA expression was determined using Novostart SYBR qPCR SuperMix Plus (novoprotein, E096-01B) according to manufacturer's instructions. According to the Gelpro32 gel image analysis program, agarose-gel electrophoresis was carried out for semi-quantitative examination of PCR results. β-actin was employed as a normalizer in the $2^{-\Delta\Delta Ct}$ relative quantitative analysis. The following primers were all used: HOTAIR, 5'-GGCAAATGTCAGAGGGTTCT-3' and 5'-TTCTTAAATTGGGCTGGGTC-3'; β-actin, 5'-CCCTGGAGAAGAGCTACGAG-3' and 5'-GGAAGGAAGGCTGGAAGAGT-3'.

Enzyme-Linked Immunosorbent Assay (ELISA)

According to the guide provided by Wuhan Genmei Technology Co., LTD. (Wuhan, China), IL-6 (catalog number: JYM0140Hu), IL-1β (catalog number: JYM0083Hu), IL-10 (catalog number: JYM0155Hu), IL-4 (catalog number: JYM0142Hu), and APN (catalog number: JYM1859Hu) levels were determined in the cell culture supernatant. Absorbance readings were measured at 450 nm using an enzyme-labeler (Rayto RT-6000, China). The contents of IL-6, IL-1β, IL-10, IL-4, and APN were calculated according to the standard curve.

Cell Counting Kit-8 (CCK-8) Assay

Cell viability was tested with a CCK-8 assay kit (BIOSS, BA00208, Beijing, China). Specifically, PCs were placed onto 96-well plates (3×10^4 cells/well) for culture until 70% and 90% confluence. Logarithmic-phase PCs were transfected as mentioned above. In each group, three wells were subjected to 0, 12, 24, 48, and 72 h of culture, respectively. Next, CCK-8 solutions were added into the plates (10 mL/well) for 1–4 h of cell incubation at 37°C. PCs viability was analyzed by detecting OD values at 450 nm.

Western Blot (WB) Analysis

To extract total proteins, cells underwent lysing with the Radio-Immunoprecipitation Assay lysis solution and 10-min centrifugation (12,000 r/min). The gel preparation kit for sodium dodecyl sulfate-polyacrylamide gel electrophoresis (SDS-PAGE) (Beyotime, Shanghai, China) was used. To produce protein samples, cells were treated with a 1:4 ratio of the 5 × SDS-PAGE protein loading buffer (10%SDS-PAGE gel, add about 50 μg of protein to each well). Samples were placed into SDS-PAGE gel wells (5–10 μL/well) subsequent to 10-min heating in a boiling water bath (Electrophoresis Apparatus, Tanon EPS300, Shanghai, China; Electrophoresis Tank, Tanon VE-180, Shanghai, China). Soak the sponge, jelly and membranes in a pre-cooled transfer buffer for 20 min, and then transfer the membranes in the order of cathode carbon plate, sponge, filter paper, jelly, membranes, filter paper, sponge and anode carbon plate (Membrane Transfer Instrument, Tanon VE-186, Shanghai, China). Following the transfer of the protein into membranes, the membranes were allowed to reach room temperature. Thereafter, they were placed into the prepared Western washing solution to remove membrane transfer solution during a 5-minute washing cycle. After being added into Western sealing solutions (5% BSA), the membranes were gently shaken for two hours at room temperature and subjected to phosphate-buffered saline containing Tween 20 washing (10 min/3 times). Primary pig antibodies were used to probe the membrane overnight at 4°C for the expression of p-AKT, PI3K, PTEN, AKT, p-PI3K, APN, ADIPOR1, and ADIPOR2. Secondary antibodies labeled with horseradish peroxidase were diluted with secondary antibody diluents (p-AKT, 1:1000, Rabbit, CST, 4060s; PI3K, 1:1000, Mouse, Abcam, ab86714; PTEN, 1:1000, Rabbit, Abcam, ab170941; AKT, 1:1000, Rabbit, CST, 4691s; p-PI3K, 1:500, Rabbit, Abcam, ab182651; APN, 1:1000, Rabbit, bioss, bs-0471R; ADIPOR1, 1:1000, Rabbit, bioss, bs-0610R; ADIPOR2, 1:1000, Rabbit, bioss, bs-0611R; GAPDH, 1:1000, Mouse, Zsbio, TA-08; Goat Anti-Mouse IgG, 1:20,000, Zsbio, ZB-2305; Goat Anti-Rabbit IgG, 1:20,000, Zsbio, ZB-2301) and incubated with the membranes for 1 h at room temperature. Following electrogenerated chemiluminescence coloring, exposure in a darkroom, fixing, and photographing, the ratio of target protein absorbance to glyceraldehyde-3-phosphate dehydrogenase absorbance was determined (Automatic exposure instrument, JS-1070P, Shanghai Peiqing Technology Co., LTD).

Immunofluorescence (IF)

The expression of p-AKT, p-PI3K, and APN was tested. Primary antibodies against p-AKT, p-PI3K, or APN was added. Subsequent to washing, secondary antibodies [goat anti-rabbit IgG (FITC), 1:400] was added. After incubation and cleaning, fluorescence microscope was used for observation and photography.

Statistical Analysis

ARM and the random walking model were utilized. IBM SPSS Statistics 26 (SPSS, Chicago, Ill, USA) and GraphPad Prism 9 software (GraphPad Software, La Jolla, CA) were adopted for data processing. Intergroup comparisons were carried out with the two-tailed Student's *t*-test or Man-Whitney U nonparametric test. Post hoc tests used for multiple comparison with Kruskal Wallis. The chi-square test was employed for comparing categorical variables. Data were depicted as mean ± standard deviation or median (quartile range). Differences were significant at $P < 0.05$.

Results

Clinical Data of Subjects

Compared with those in HC individuals, ESR, TC, TG, IgA, and C3 levels in OA patients were conspicuously higher ($P < 0.05$). After JQP treatment, hs-CRP, VAS, TG, and SAS in OA patients decreased considerably ($P < 0.05$), and no remarkable differences were noted in age and gender ($P > 0.05$) (Table 1).

Expression of HOTAIR and Changes in Inflammation and APN

qRT-PCR revealed that the PBMCs in OA patients had higher levels of HOTAIR expression. The ELISA technique test revealed that before therapy, PBMCs from OA patients had higher TNF-α levels and lower IL-10 and APN levels than those from HC individuals. Following JQP treatment, HOTAIR expression was substantially lowered (Figure 1A), and inflammation and APN were reversed (Figure 1B–D).

Association Rule Analysis of HOTAIR Levels with Immune Inflammation and Lipid Metabolism in OA Patients

To clarify the relationship between JQP and HOTAIR and changes in inflammatory and lipid metabolism indicators, we performed association rule analysis to identify the confidence, support, and improvement of JQP use and clinical characteristics of OA patients. JQP shows a strong correlation with improved hs-CRP, C3, TNF-α, IgA, IgM, IgG, C4, and TC, according to the analysis results. Both the support and the confidence levels exceed 15% and 55%, respectively. (Table 2).

JQP Intervention Was Associated with Long-Term Improvements in Clinical Indicators

To determine the role of JQP in OA treatment, a random walking model was adopted to quantitatively evaluate the improvement of clinical indicators. The results included maximum random volatility, walking steps, positive walk growth rate, positive walk growth rate for each index, improvement factor, and ratio (Table 3). Each step of improvement of C4, IgA, IgG, and IgM required 12.48, 8.2, 10.63, and 0.75 steps, which were clinically relevant in the model evaluation. Data displayed that JQP used had a long-term relationship with improvements in C4, IgA, IgG, and IgM levels (Figure 2).

Table 1 Clinical Characteristics of Subjects

Index	HC (n=20)	OA (n=30)	
		Before Treatment	After Treatment
Gender (female)	12	17[c]	17[c]
Age (years)	54.65 ± 9.35	55.87 ± 10.06[d]	55.87 ± 10.06[a]
ESR (mm/h)	9.35 ± 5.86	17.5 (8.0, 32.5)[b]**	20 (10.75, 30.25)[b]
hs-CRP (mg/L)	1.34 (0.89, 3.96)	1.62 (0.8, 7.73)[b]	1.53 (0.36, 4.31)[b#]
TC (mmol/L)	2.01 ± 0.67	4.75 (3.91, 5.45)[b]**	4.66 (4.02, 5.25)[b]
TG (mmol/L)	0.62 ± 0.41	1.4 (1.15, 1.68)[b]**	1.07 (0.74, 1.22)[b##]
IgA (g/L)	1.77 ± 0.64	2.33 ± 0.85[d]*	2.30 ± 0.89[a]
IgG (g/L)	8.21 (7.96, 9.30)	9.58 (7.68, 10.72)[b]	8.99 (7.8, 10.78)[b]
IgM (g/L)	0.89 (0.54, 1.78)	1.14 (0.76, 1.56)[b]	1.02 (0.75, 1.51)[b]
C3 (g/L)	1.07 (0.96, 1.10)	1.13 ± 0.18[b]*	1.14 ± 0.19[a]
SDS score	NA	51.79 ± 8.42	50.6 ± 6.25[a]
VAS score	NA	6 (5, 6)	1 (1, 2)[b##]
SAS score	NA	42.5 (35.93, 47.5)	40 (37.18, 43.75)[b#]

Notes: Clinical characteristics of subjects. [a]Student's *t*-test. [b]Nonparametric test (median). [c]Chi-square test. [d]Two independent samples *t*-test. *$P < 0.05$, **$P < 0.01$ vs HC group; #$P < 0.05$, ##$P < 0.01$, vs before treatment.

Abbreviations: HC, healthy control; OA, Osteoarthritis; hs-CRP, hyper-sensitivity C-reactive protein; C3, complement C3; IgA, G, M, immunoglobulin A, G, M; ESR, erythrocyte sedimentation rate; TC, Total cholesterol; TG, Triglyceride; SAS, Self Rating Anxiety Scale; SDS, Self Rating Depression Scale; VAS, visual analogue scale. NA, not applicable.

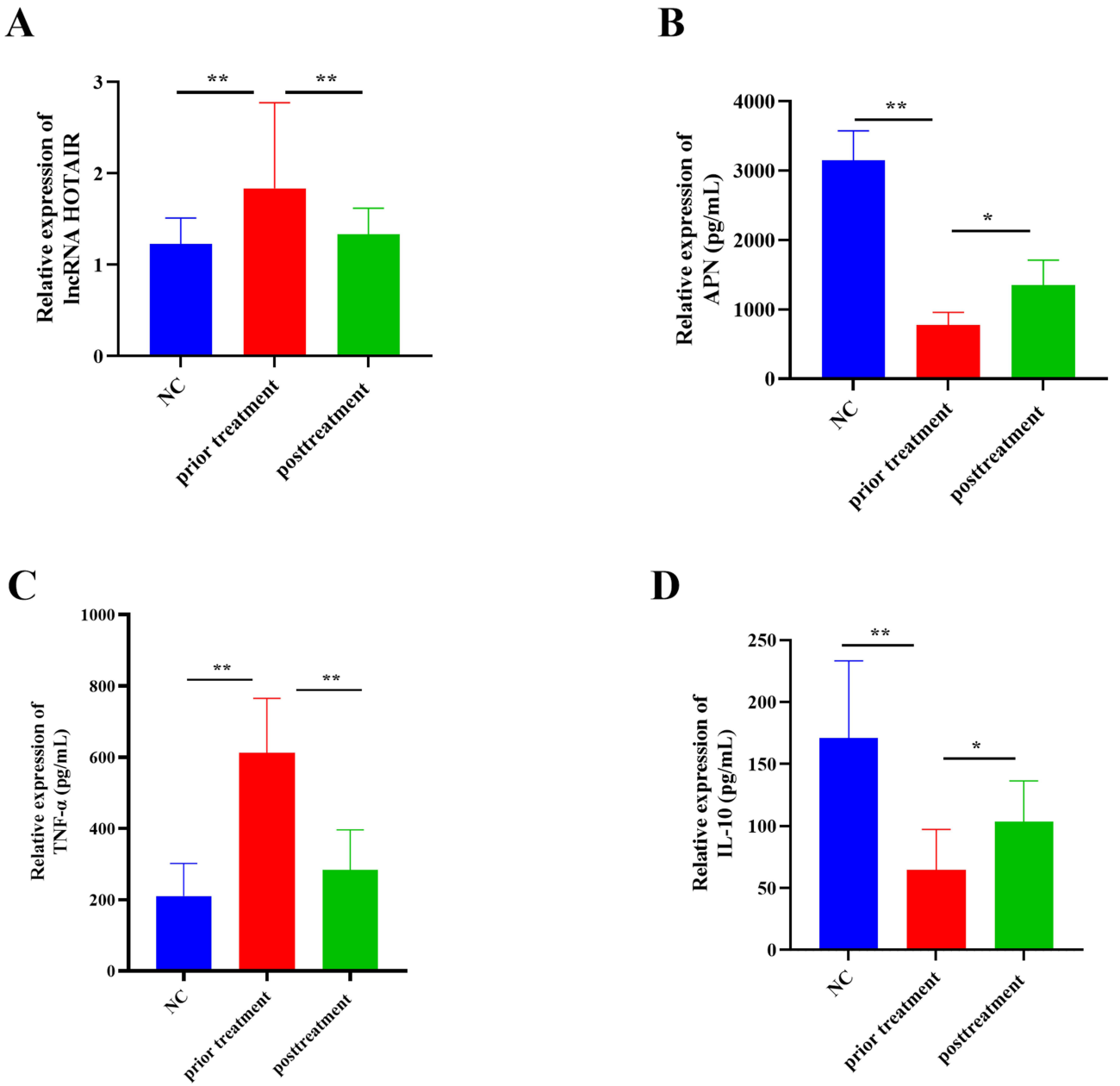

Figure 1 Expression of HOTAIR and changes in inflammation and APN. (**A**) RT-qPCR to test HOTAIR expression. (**B**–**D**) ELISA to analyze TNF-α, IL-10, and APN levels. All experiments were replicated thrice. *P < 0.05, **P < 0.01.
Abbreviations: NC, Control group; HOTAIR, Lnc RNA HOTAIR; APN, Adiponectin; TNF-α, Tumornecrosisfactor-α; IL-10, Interleukin-10.

JQP Active Ingredients

Totally, 164 active components of JQP were filtered by ADME to meet the criteria of OB value ≥ 30% and DL value ≥0.18. The information of the top 20 TCM active ingredients in OB value is shown in the following table (Table 4).

Potential Target Identification and Compound-Target Network Construction

Totally, 1635 target proteins of the 164 candidates active components were yielded by searching the TCMSP database. Subsequent to standardization and de-duplication, 216 intersected targets were attained. The number of OA-related targets in DrugBank, Genecards, TTD, and OMIM were 286, 3099, 89, and 25, respectively. Following de-duplication, 863 OA-related targets were acquired. Based on the above results, 98 potential targets of JQP in OA treatment were

Table 2 Association Rule Analysis of JQP with Clinical Characteristics of OA Patients

The Former	The Latter	Support (%)	Confidence (%)	Lift
JQP	hs-CRP ↓	20.00	71.42	1.42
JQP	C3↓	24.00	85.71	1.33
JQP	TNF-α↓	18.00	70.42	1.01
JQP	IgA↓	20.00	71.42	1.27
JQP	IgM↓	20.00	71.42	1.08
JQP	IgG↓	18.00	64.28	1.07
JQP	C4↓	18.00	64.28	1.10
JQP	TC↓	16.00	57.14	1.02

Note: Association rule analysis of JQP with clinical characteristics of OA patients.
Abbreviations: JQP, Jianpi Qingre Tongluo Prescription; hs-CRP, hyper-sensitivity C-reactive protein; C3, complement C3; C4, complement C4; IgA, G, M, immunoglobulin A, G, M; TC, Total cholesterol; TNF-α, Tumornecrosisfactor-α.

Table 3 The Random Walk Evaluation Model of Laboratory Indicators of OA Patients Treated with JQP

Indicators	Maximum Random Volatility	Walking Steps	Positive Walk Growth Rate	Positive Walk Growth Rate	Improvement Factor	Ratio
IgA	35	287	0.122	0.2066±0.0759	0.4167	8.2
IgM	16	12	1.3333	0.3525±0.1946	0.1905	0.75
IgG	27	287	0.0941	0.2843±0.1373	0.3214	10.63
C4	23	287	0.0801	0.1874±0.1459	0.2738	12.48

Note: The random walk evaluation model of laboratory indicators of OA patients treated with JQP.
Abbreviations: C4, complement C4; IgA, G, M, immunoglobulin A, G, M.

harvested through the Venn diagram (Figure 3). To determine the relationship between the compounds in eight Chinese herbal medicines of JQP and the corresponding targets, Cytoscape 3.8.2 software was adopted for developing a drug-compound-target network (Figure 4). The 365 nodes were connected by 1726 edges, in which the green arrow nodes

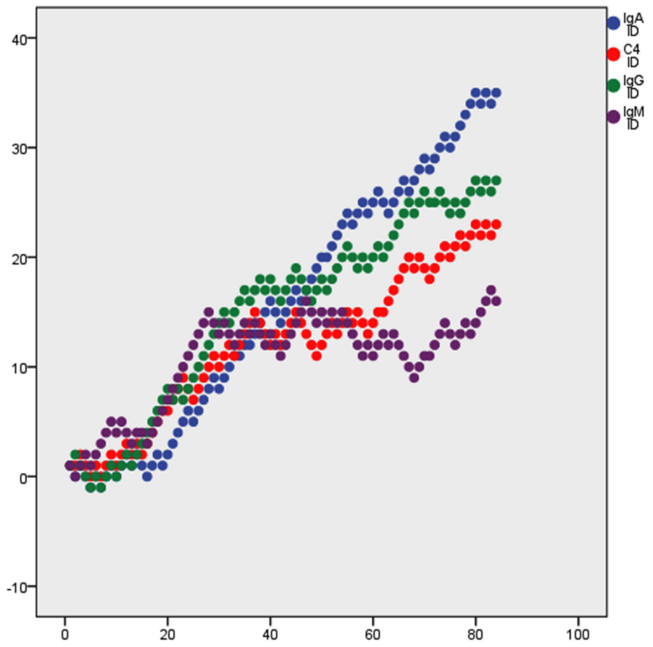

Figure 2 Random walking analysis of JQP and clinical indicators.
Abbreviations: JQP, Jianpi Qingre Tongluo Prescription; C4, complement C4; IgA, G, M, immunoglobulin A, G, M.

Table 4 Active Ingredient Information of JQP

MOL ID	Molecular	OB (%)	DL
MOL001371	Populoside_qt	108.89	0.2
MOL002934	NEOBAICALEIN	104.34	0.44
MOL001351	Gibberellin A44	101.61	0.54
MOL001348	Gibberellin 17	94.64	0.49
MOL001353	GA60	93.17	0.53
MOL002937	DIHYDROOROXYLIN	66.06	0.23
MOL004561	Sudan III	84.07	0.59
MOL001360	GA77	87.89	0.53
MOL001340	GA120	84.85	0.45
MOL001339	GA119	76.36	0.49
MOL002932	Panicolin	76.26	0.29
MOL012246	5,7,4'-trihydroxy-8-methoxyflavanone	74.24	0.26
MOL001342	GA121-isolactone	72.7	0.54
MOL002927	Skullcapflavone II	69.51	0.44
MOL001358	Gibberellin 7	73.8	0.5
MOL002911	2,6,2',4'-tetrahydroxy-6'-methoxychaleone	69.04	0.22
MOL001349	4a-formyl-7alpha-hydroxy-1-methyl-8-methylidene-4aalpha,4bbeta-gibbane-1alpha,10beta-dicarboxylic acid	88.6	0.46
MOL001344	GA122-isolactone	88.11	0.54
MOL001329	2,3-didehydro GA77	88.08	0.53
MOL001361	GA87	68.85	0.57

represented the eight Chinese herbal medicines in JQP; the orange diamond nodes represented potential drug targets; and the pink octagon nodes represented active compounds.

The top 5 components of the degree value are quercetin, kaempferol, Beta-sitosterol, Stigmasterol and hederagenin, which have multiple therapeutic targets related to OA and may be implicated in OA treatment. The core active ingredients of JQP for OA treatment are listed in Table 5.

Construction of PPI Network

The PPI network based on the data file of the STRING database was constructed by using Cytoscape3.8.2 (Figure 5), comprising 98 nodes. The mean Degree value of nodes in the network was 42.2, with a mean center clustering coefficient

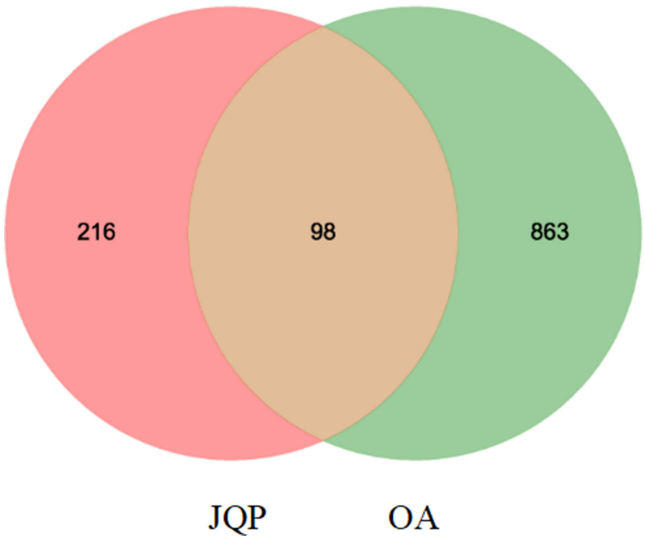

Figure 3 Venn diagram of the target genes for JQP and OA.

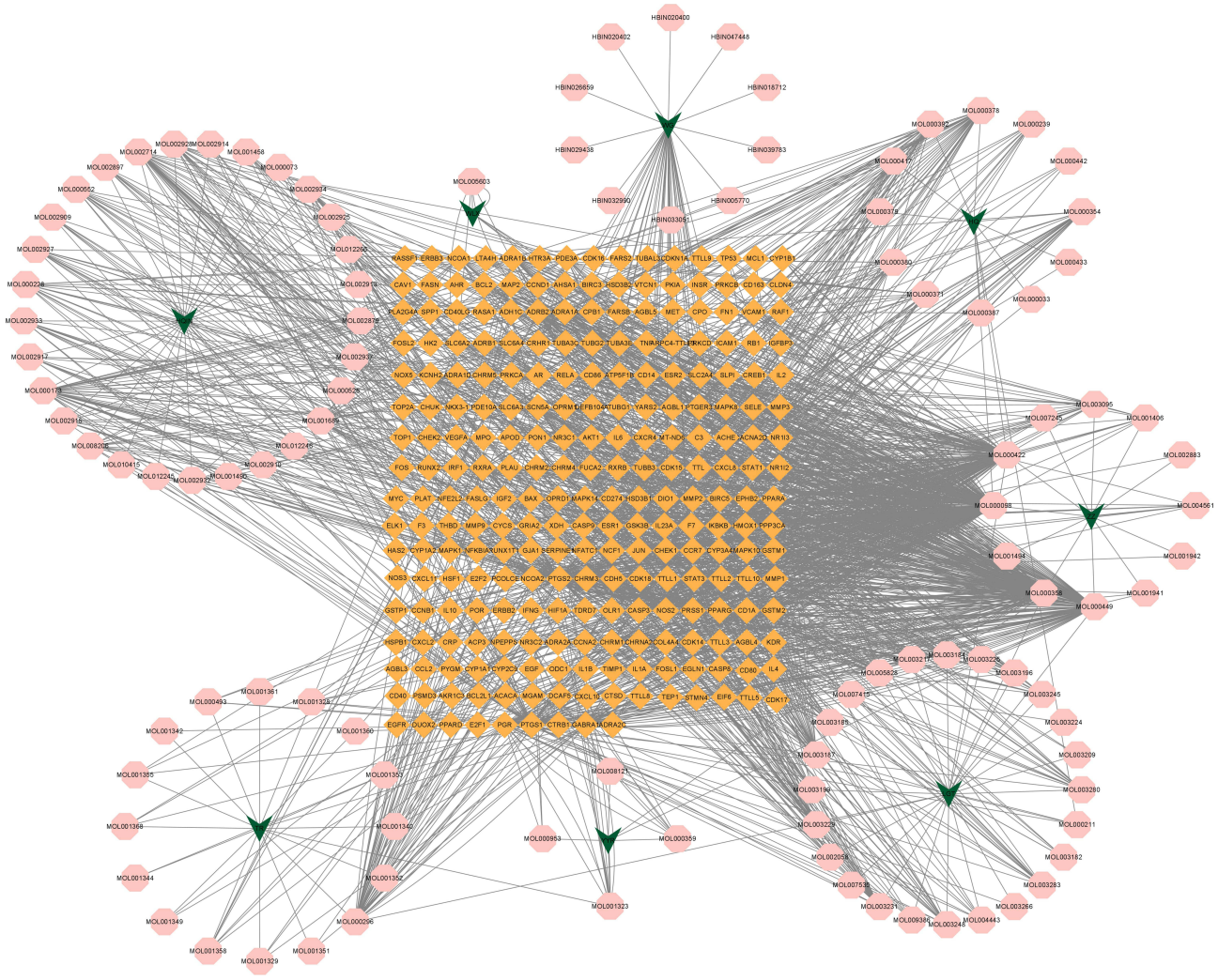

Figure 4 Network of Drug-Compound-Target of JQP. LGT: Tripterygium wilfordii Hook. f, WLX: Clematis chinensis Osbeck, ZZ: Gardenia jasminoides J. Ellis, HQIN: Scutellaria baicalensis Georgi, WG: Scolopendra subspinipes mutilans L. Koch, YYR: Coix lacryma-jobi L, TR: Juglans regia L, HQ: Astragalus mongholicus Bunge. Green arrow nodes: the eight Chinese herbal medicines in JQP; Orange diamond nodes: potential drug targets; pink octagon nodes: active compounds.

of 0.743. The top targets in Degree value were acquired as the core targets including TNF, IL-6, IL-1β, and AKT1 (Table 6).

GO and KEGG Pathway Enrichment Analyses

GO and KEGG enrichment analyses were performed on the 98 target genes by using the Metascape database to further analyze the biological effect, cellular localization, pathway, and function of the 98 targets of JQP in OA treatment. The

Table 5 The Core Active Ingredient of JQP for the Treatment of OA

Chinese Medicine Name	Mol ID	Molecule Name	Degree
Gardenia jasminoides J.Ellis, Astragalus mongholicus Bunge	MOL000098	Quercetin	254
Gardenia jasminoides J.Ellis, Astragalus mongholicus Bunge, Tripterygium wilfordii Hook. f	MOL000422	Kaempferol	150
Scutellaria baicalensis Georgi, Clematis chinensis Osbeck, Gardenia jasminoides J.Ellis, Juglans regia L, Tripterygium wilfordii Hook. f	MOL000358	Beta-sitosterol	135
Scutellaria baicalensis Georgi, Clematis chinensis Osbeck, Gardenia jasminoides J.Ellis, Coix lacryma-jobi L, Tripterygium wilfordii Hook. f	MOL000449	Stigmasterol	115
Juglans regia L, Astragalus mongholicus Bunge	MOL000296	Hederagenin	45

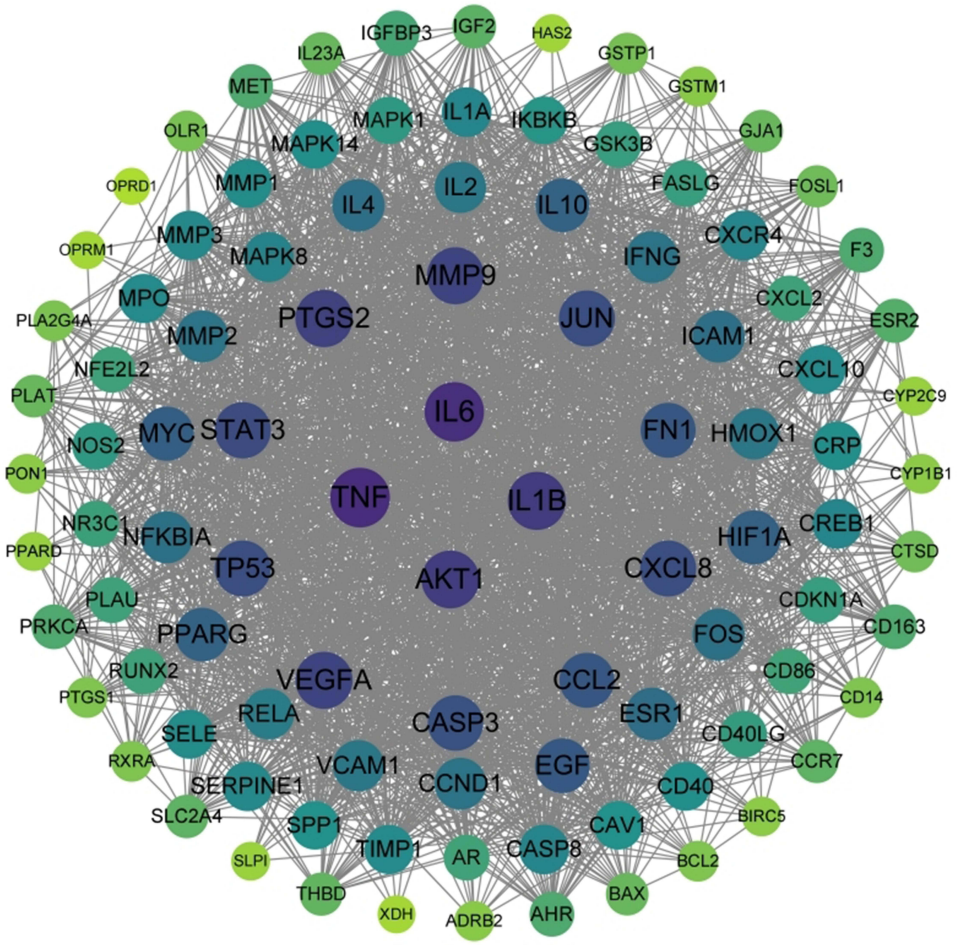

Figure 5 Core protein-protein interaction network.

results predominantly covered three parts: BP, CC, and MF. The top 20 enriched GO items were listed in ascending order of P-value. The abscissa was the false discovery rate (FDR) and the left side of the ordinate was the GO classification. The size of circles represented the number of genes in each GO term; the color depth represented the enrichment P value, and the redder the circle, the more significant the enrichment (Figure 6). GO enrichment analysis results for BP showed that GO items that responded to lipopolysaccharide, inorganic substance, and wounding, and positively regulated cell migration and cellular response to organic cyclic compounds were enriched. The results for CC showed that GO items, such as membrane raft, side of the membrane, vesicle lumen, transcription regulator complex, and receptor complex were enriched. The results for MF showed that GO items, such as cytokine receptor binding, protein kinase binding, transcription factor binding, protein and homodimerization activity, and protein domain specific binding were enriched. The top 20 enriched KEGG pathways were listed in an ascending order of *P*-value. The abscissa was the FDR and the left side of the ordinate was the name of the KEGG pathways. The size of circles represented the number of genes in the

Table 6 The Core Targets of JQP in OA Treatment

Gene Name	Target Name	Degree
TNF	Tumor necrosis factor	88
IL6	Interleukin-6	87
IL1B	Interleukin-1 beta	82
AKT1	Serine/threonine-protein kinase AKT	81

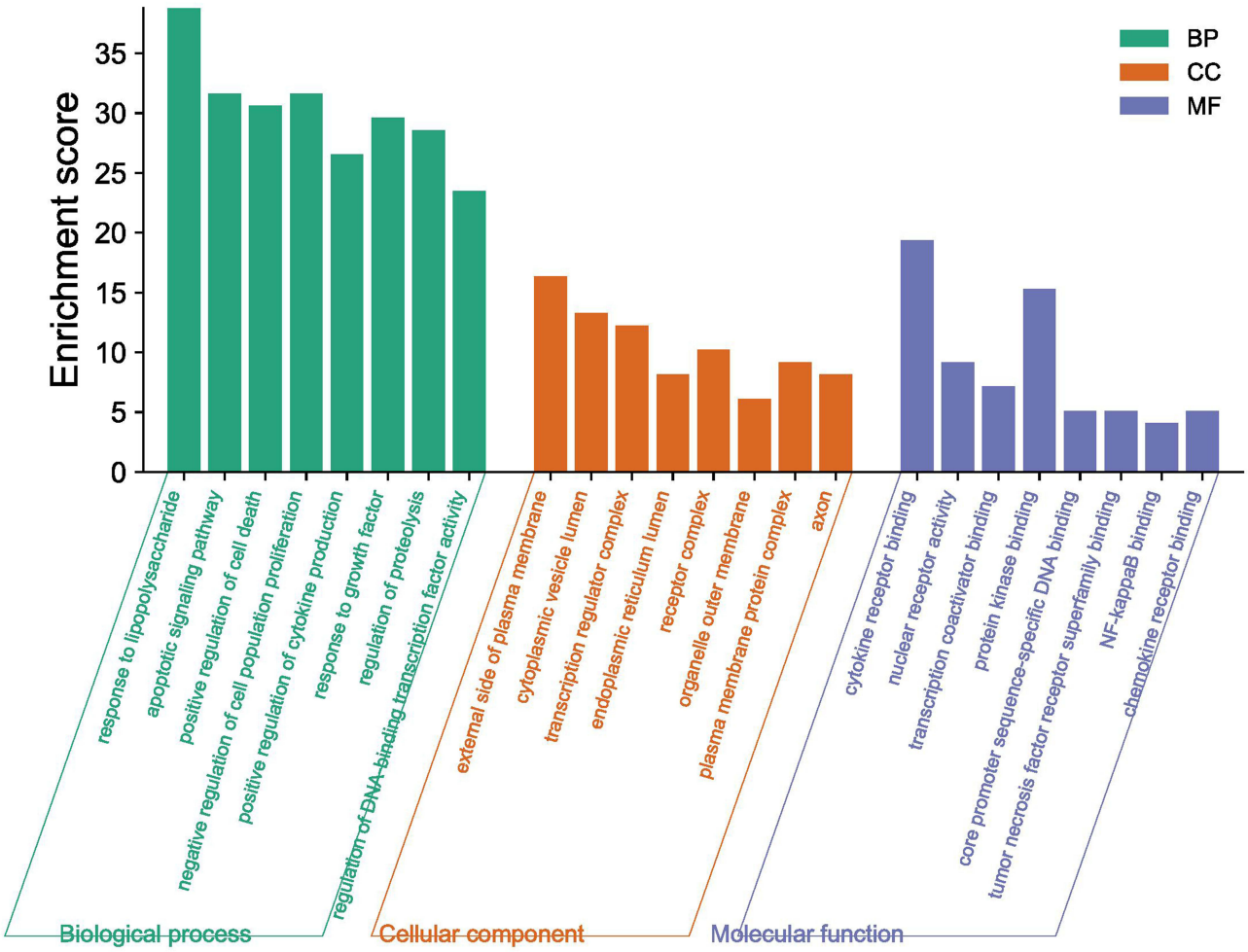

Figure 6 The enriched GO items.

pathways; the color depth represented the enrichment P value, and the redder the circle, the more significant the enrichment (Figure 7). KEGG enrichment analysis results showed that pathways like PI3K-AKT, MAPK, apoptosis, TNF, and IL-17 were enriched.

Molecular Docking

Combined with the previous results of UPLC-MS/MS and HPLC fingerprinting, we summarized the main active ingredients of JQP, and docking with key targets. The result is the heatmap (Figure 8). Higher binding activities between compounds and target protein receptors signified lower binding energies. The results showed that the binding energies of the main active components of JQP and the key targets for the treatment of OA were all lower than −5 kcal/mol, except danshensu and AKT1. In addition, we visualized the three docking results with the lowest binding energy (AKT1 and puerarin was −9.2 kcal/mol, AKT1 and salvianolic acid B was −9.3 kcal/mol, TNF and salvianolic acid B was −9.1 kcal/mol) (Figure 9).

Effects of PBMCs on Levels of HOTAIR, IL-1β, IL-6, IL-4, IL-10, and APN in CH

Combined with network pharmacology and molecular docking, the mechanism of JQP in OA treatment was further explored. RT-qPCR data (Figure 10A) revealed that PBMCs could promote HOTAIR expression in CHs from OA patients. ELISA data (Figure 10B–F) suggested that PBMCs could promote IL-1β and IL-6 levels while decreasing IL-4, IL-10, and APN levels in CHs from OA patients.

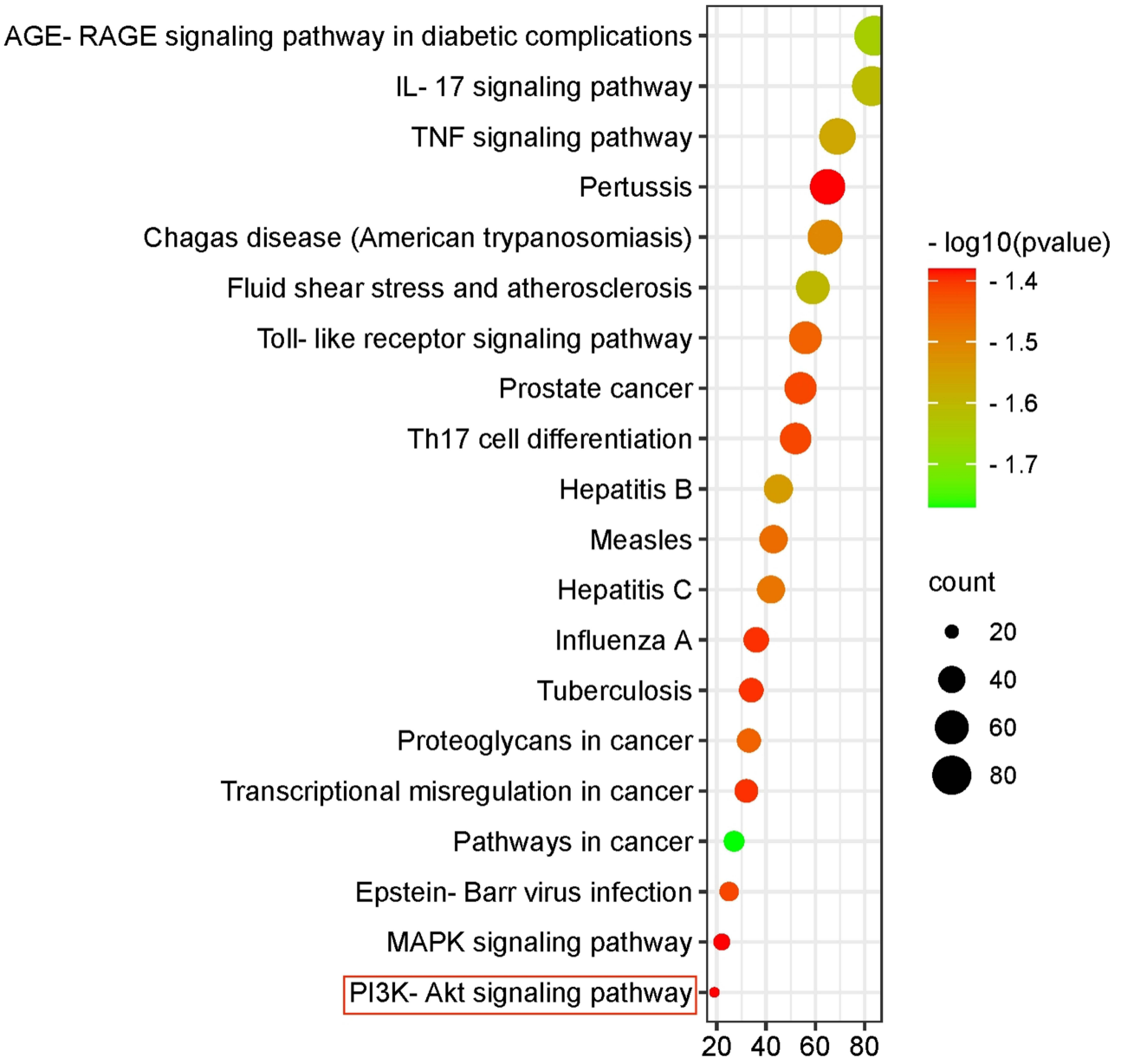

Figure 7 The enriched KEGG pathways.

Effects of HOTAIR on Levels of APN and PI3K/AKT Pathway in PC

First, RT-qPCR was employed to screen small interfering plasmids (Figure 11A and B), and then CCK-8 was utilized to measure CH viability. The results showed that overexpression of HOTAIR decreased the viability of PC cells, while silencing of HOTAIR promoted the viability of PC cells (Figure 11C). Semi-quantitative immunofluorescence assay found that HOTAIR overexpression augmented phosphorylation of PI3K, AKT and diminished APN levels (Figure 11I–K). However, after knock downing HOTAIR, PI3K and AKT phosphorylation declined and APN levels rose. The same results were obtained by quantitative detection with WB method (Figure 11D). It suggests that changes in HOTAIR levels can cause changes in PI3K/AKT and APN levels. ELISA data (Figure 11E–H) exhibited that HOTAIR overexpression could promote IL-1β and IL-6 levels (Figure 11E and H) and lower IL-4 and IL-10 levels (Figure 11F and G) in PC. Meanwhile, opposite trends were noted after knockdown of HOTAIR (Figure 11F and G).

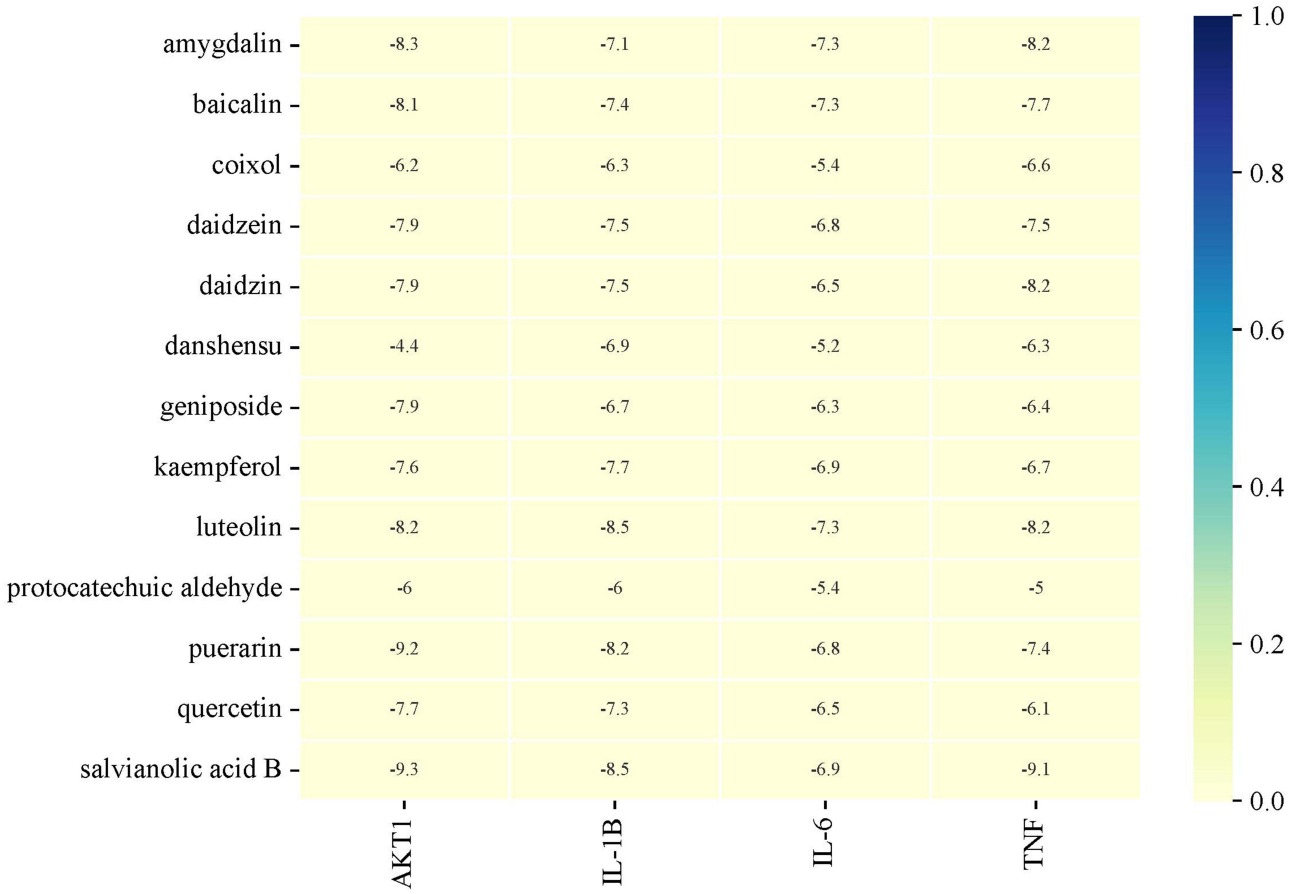

Figure 8 The heatmap of docking scores of key targets combining to active compounds in JQP.

Impacts of HOTAIR on Cell Viability and IL-1β, IL-6, IL-4, IL-10, and APN Levels Through PI3K/AKT Pathway in PC

First, CCK-8 results manifested that PI3K/AKT inhibitor can promote CH viability, and then overexpression of HOTAIR can reverse this effect (Figure 12A). Through semi-quantitative immunofluorescence assay found that PI3K/AKT inhibitor decrease phosphorylation of PI3K and AKT, however, there was no effect on the level of APN. Overexpression of HOTAIR can increase phosphorylation of AKT, meanwhile, decreasing level of APN (Figure 12G–I), the same results were obtained by quantitative detection with WB method (Figure 12B). It suggests that changes in PI3K/AKT pathway levels cannot cause changes in APN levels. In addition, HOTAIR may inhibit APN levels. ELISA data (Figure 12C–F) displayed that PI3K/AKT inhibitor diminished IL-1β and IL-6 levels (Figure 12D and F) and promote IL-4 and IL-10 levels (Figure 12C and E) in CHs, and meanwhile, overexpression of HOTAIR can reverse this effect. In summary, the function of HOTAIR in reducing cell viability, up-regulating pro-inflammatory factors, and down-regulating anti-inflammatory factors may be achieved by orchestrating APN and PI3K/AKT pathway.

Impacts of HOTAIR on PI3K/AKT Pathway, Cell Viability and IL-1β, IL-6, IL-4, IL-10 Levels via Regulating APN in PC

First, CCK-8 data demonstrated that overexpression of APN can promote CH viability, and then overexpression of HOTAIR can reverse this effect (Figure 13A). PCR results show that not only HOTAIR level can regulate APN level but also overexpression of APN may promote HOTAIR expression through constructing overexpression plasmids of HOTAIR and APN (Figure 13B). Through semi-quantitative immunofluorescence assay found that overexpression of APN decreased phosphorylation of PI3K

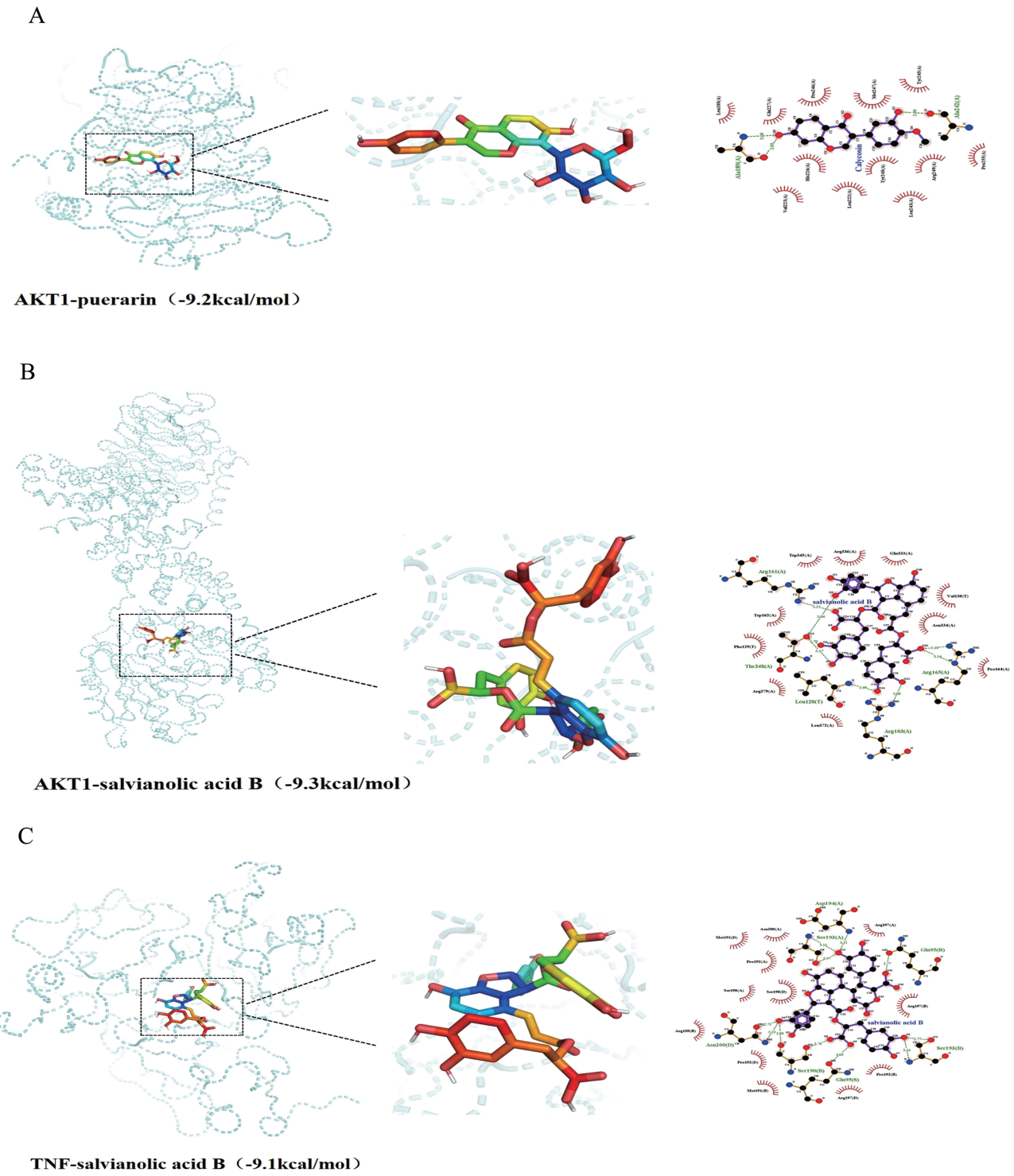

Figure 9 The representative docking complex of key targets and compounds of JQP in OA treatment, (**A**) AKT1 and puerarin; (**B**) AKT1 and salvianolic acid B; (**C**) TNF and salvianolic acid B.

and AKT. Meanwhile, HOTAIR overexpression not only restrained APN expression but also weakened the repressive effect of APN on PI3K/AKT pathway, mainly AKT phosphorylation, to a certain extent (Figure 13H–J). The same results were obtained by quantitative detection with WB (Figure 13C). ELISA data (Figure 13D–G) depicted that APN overexpression lowered IL-1β and IL-6 levels (Figure 13D and G) and augmented IL-4 and IL-10 levels (Figure 13E and F) in CHs, whilst overexpression of

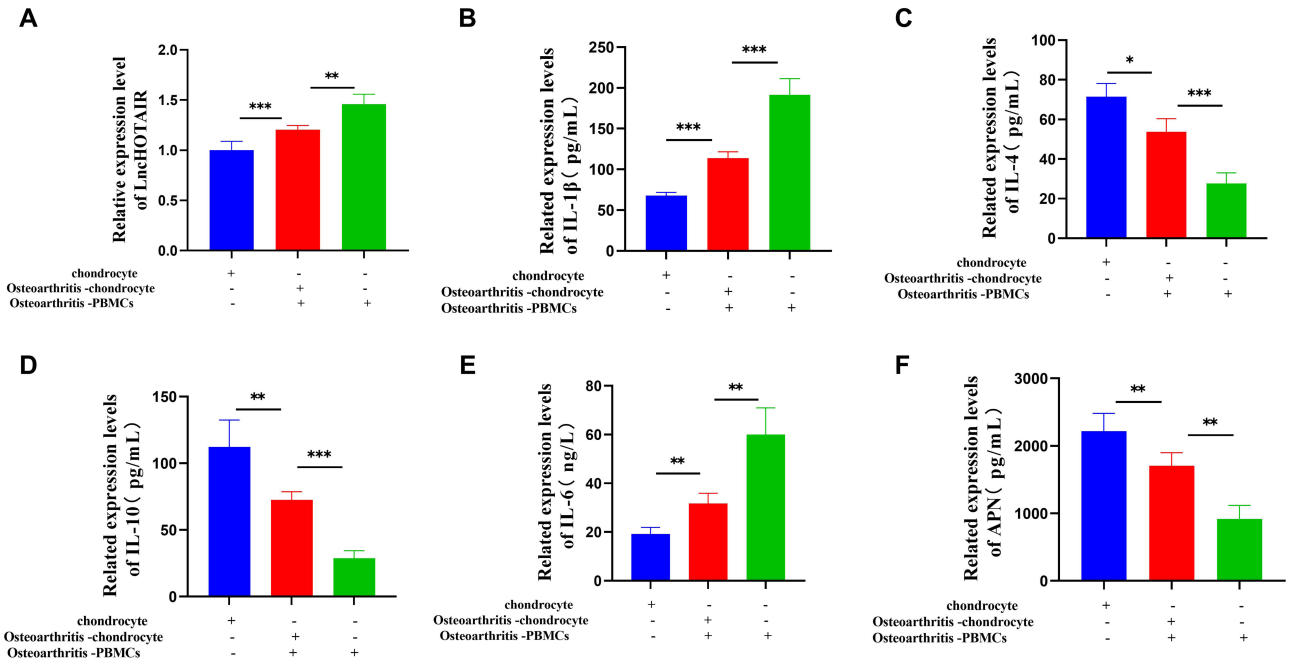

Figure 10 RT-qPCR to examine HOTAIR expression (**A**); ELISA to test IL-1β, IL-6, IL-4, IL-10, APN levels (**B-F**). *** P < 0.001; ** P < 0.01; * P < 0.05.
Abbreviations: PBMCs, Peripheral Blood Mononuclear Cells; LncHOTAIR, Lnc RNA HOTAIR; APN, Adiponectin; IL-1β/4/6/10, Interleukin-1β/4/6/10.

HOTAIR nullified this effect. In summary, the functions of APN in promoting cell viability and anti-inflammatory factors and repressing phosphorylation of PI3K/AKT pathway and pro-inflammatory factors may be regulated by HOTAIR.

Salvage Impacts of JQP on APN Level, PI3K/AKT Pathway, Cell Viability, and Inflammatory Factors in PC

First, CCK-8 data showed that JQP intervention could not only inhibit the CH inhibition of HOTAIR but also directly promote the proliferation activity of CHs (Figure 14A). PCR results show that JQP could inhibit HOTAIR expression (Figure 14B). Through semi-quantitative immunofluorescence assay, JQP can not only reduce p-PI3K and p-AKT levels and increase APN levels but also inhibit the promotion of HOTAIR on PI3K/AKT pathway and its inhibition on APN (Figure 14G–I). The same results were obtained by quantitative detection with WB (Figure 14C). This may mean that JQP reduces p-PI3K and p-AKT levels and increases APN levels by inhibiting HOTAIR expression. ELISA data (Figure 14D–G) exhibited that JQP can inhibit the promotion of HOTAIR on IL-1β and IL-6 levels (Figure 14D and G) and its inhibition on IL-4 and IL-10 levels (Figure 14E and F) in CHs. They may be achieved by inhibiting the overexpression of HOTAIR.

Discussion

JQP has been broadly utilized in clinical practice. The current research first validated the clinical efficacy of JQP through clinical data mining and then probed pharmacological mechanisms underpinning JQP decoction in OA treatment via systemic pharmacological analyses and experiments. Nevertheless, we have failed to find many references about the mechanism of JQP in OA treatment given the absence of research methods for the compound preparation of JQP decoction in the early stage. Reportedly, JQP decoction carries a marked effect of ameliorating foot swelling and pain in arthritis[44,45] and diminishing inflammatory mediator levels in patients.[41,46] More importantly, the treatment features of XFC are mainly to support positive qi, and take into account dispelling wind, clearing collaterals and relieving pain. The treatment characteristics of HQC are mainly to clear heat and remove dampness, taking into account the spleen and stomach. We were surprised to find that the combination of the two has significant clinical efficacy, which may be related to the mixed syndrome type of clinical OA. Considering the complexity of capsule preparation process and the previous research basis of the two drugs, it is necessary to design a large number of clinical randomized controlled trials and

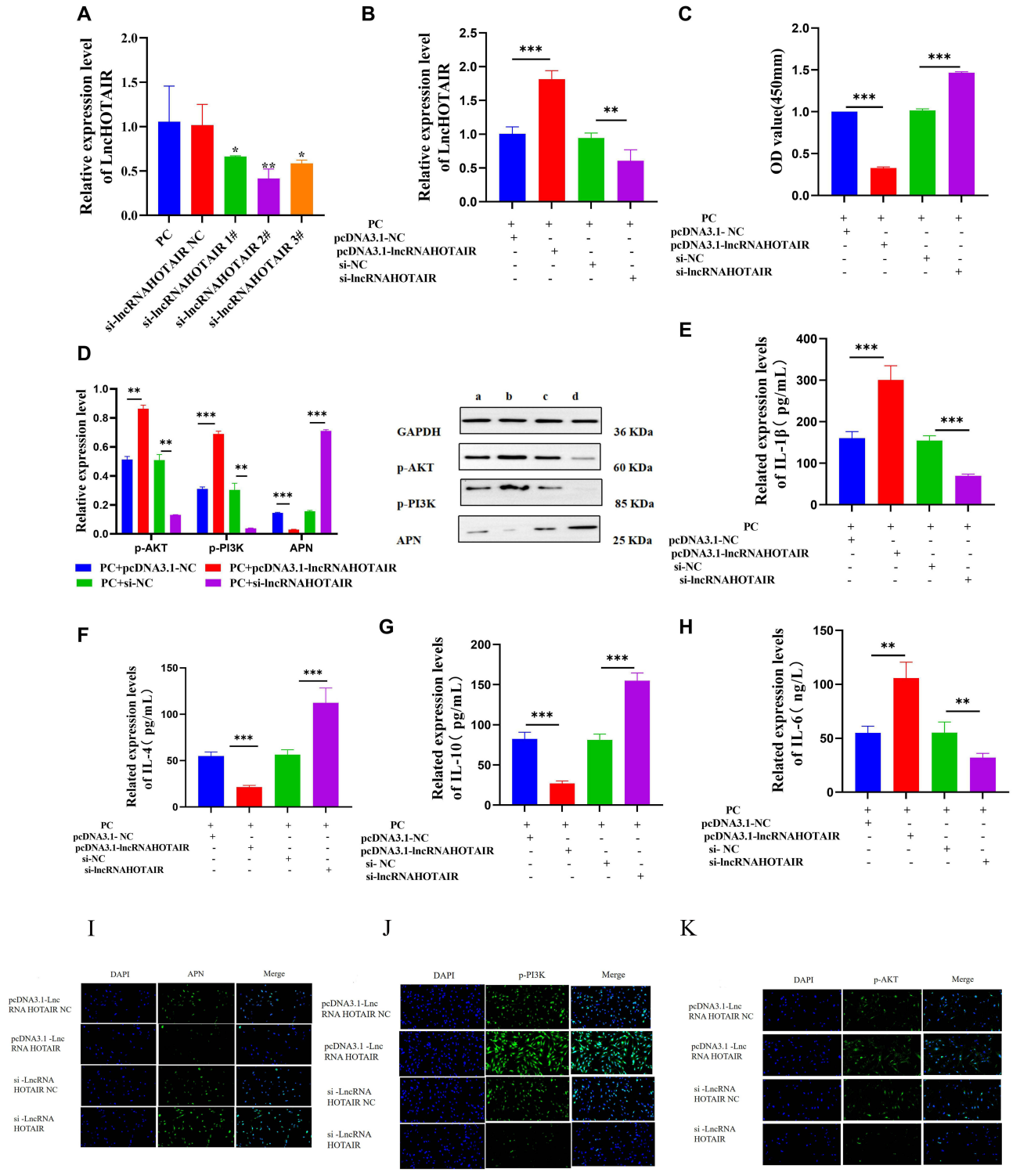

Figure 1 RT-qPCR to check HOTAIR expression (**A** and **B**); CCK-8 assay to analyze PC viability (**C**); WB to test phosphorylation of PI3K and AKT and levels of APN (**D**); ELISA to determine IL-1β, IL-6, IL-4, IL-10, and APN levels (**E**–**H**); Semi-quantitative levels of APN, p-PI3K, and p-AKT detected with immunofluorescence (**I**–**K**). *** P < 0.001; ** P < 0.01; * P < 0.05.

Abbreviations: LncHOTAIR, Lnc RNA HOTAIR; PC, OA-PBMCs (Osteoarthritis-Peripheral Blood Mononuclear Cells) +OA-CH (Osteoarthritis-chondrocytes); APN, Adiponectin; IL-1β/4/6/10, Interleukin-1β/4/6/10.

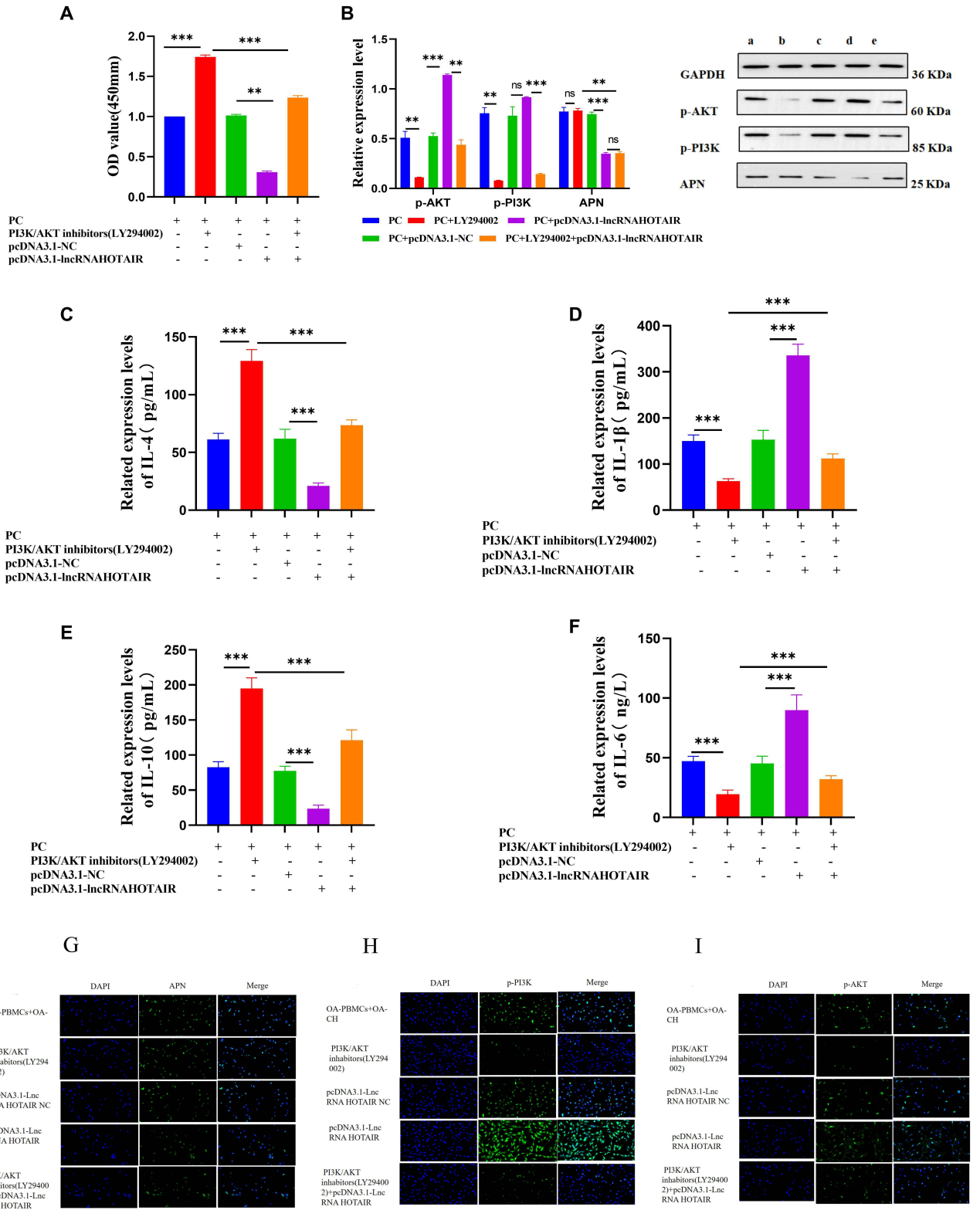

Figure 12 CCK-8 assay to examine CH viability (**A**); Phosphorylation of PI3K and AKT and level of APN measured with WB (**B**); IL-1β, IL-6, IL-4, IL-10, and APN levels tested with ELISA (**C**–**F**); Semi-quantitative levels of APN, p-PI3K, and p-AKT checked with immunofluorescence (**G**–**I**). *** $P < 0.001$; ** $P < 0.01$.

Abbreviations: PC, OA-PBMCs (Osteoarthritis-Peripheral Blood Mononuclear Cells) +OA-CH (Osteoarthritis-chondrocytes); APN, Adiponectin; IL-1β/4/6/10, Interleukin-1β/4/6/10; ns, No statistical significance.

https://doi.org/10.2147/IJGM.S466148 DovePress

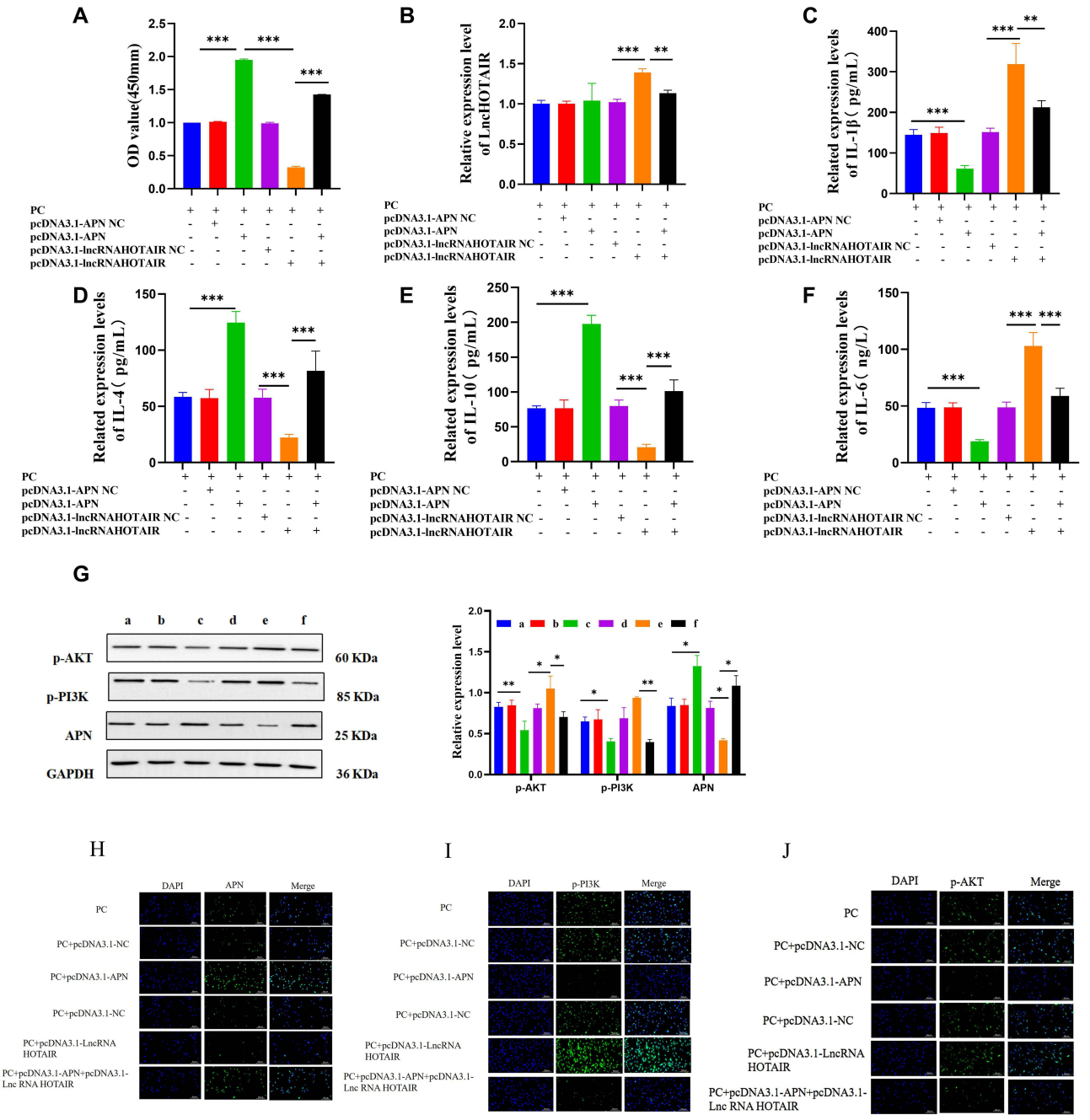

Figure 13 CH viability examined with CCK-8 assay (**A**); HOTAIR expression measured with PCR (**B**); Level of IL-1β, IL-6, IL-4, IL-10, and APN checked with ELISA (**D-F**); Phosphorylation of PI3K and AKT and level of APN tested with WB (**G**); Semi-quantitative levels of APN, p-PI3K, and p-AKT detected with immunofluorescence (**H-J**). ***$P < 0.001$; **$P < 0.01$; *$P < 0.05$.

Abbreviations: LncHOTAIR, Lnc RNA HOTAIR; PC, OA-PBMCs (Osteoarthritis-Peripheral Blood Mononuclear Cells) +OA-CH (Osteoarthritis-chondrocytes); APN, Adiponectin; IL-1β/4/6/10, Interleukin-1β/4/6/10.

in vivo and in vitro experiments to compare the advantages and disadvantages of single drug and combined drug, and to determine whether the combination of the two prescriptions is necessary.

Systemic pharmacology is a new approach wherein bioinformatics was employed to predict and identify multiple drug targets and interactions in diseases.[47] In our research, the potential targets and pathways of JQP decoction in OA treatment were also successfully predicted with the utilization of systemic pharmacology. According to our network analysis results and the previous results of UPLC-MS/MS and HPLC fingerprinting, core node compounds, such as

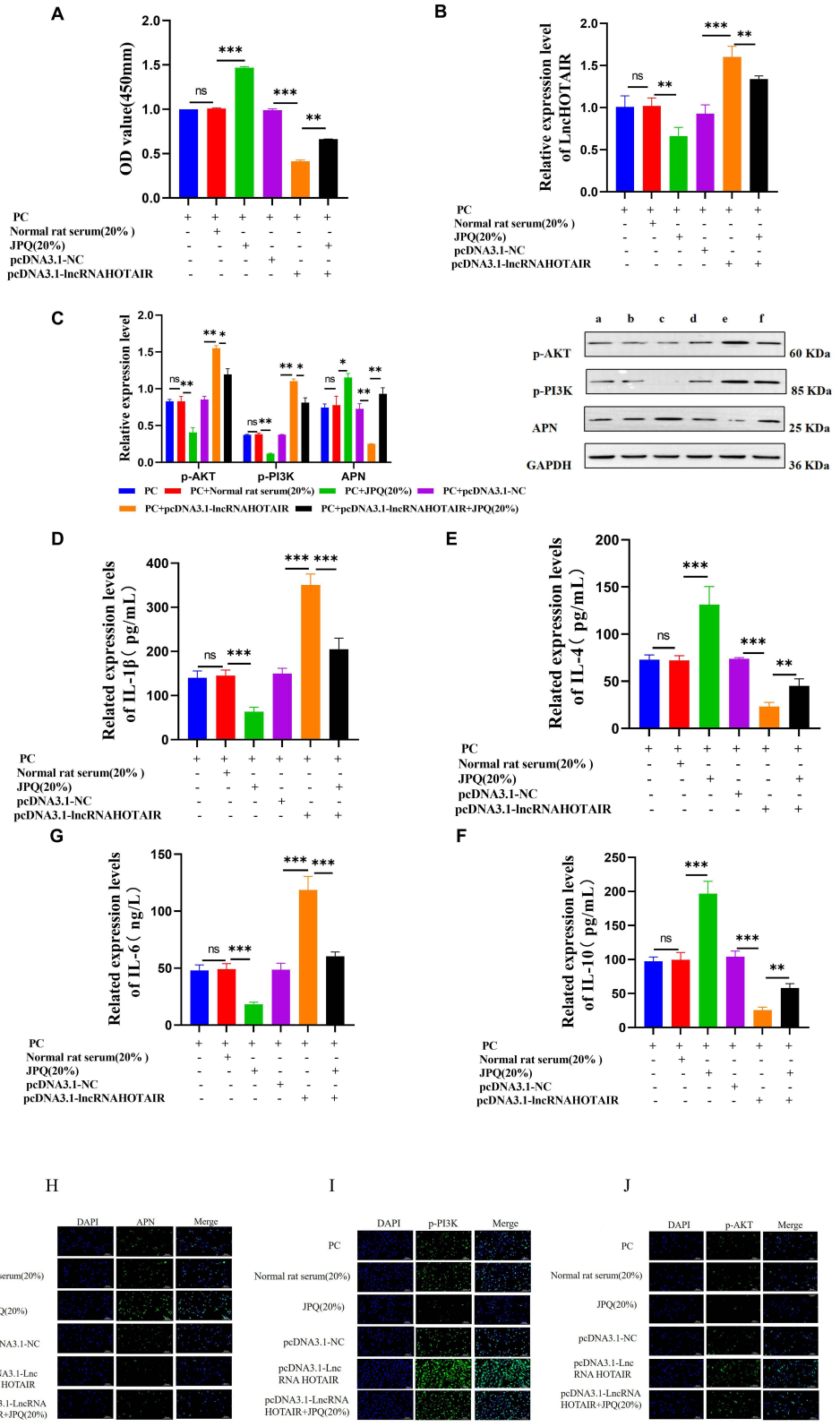

Figure 14 CH viability measured with CCK-8 assay (**A**); HOTAIR levels tested with PCR (**B**); Phosphorylation of PI3K and AKT and level of APN checked with WB (**C**); IL-1β, IL-6, IL-4, IL-10, and APN levels examined with ELISA (**D-G**); Semi-quantitative levels of APN, p-PI3K, and p-AKT determined with immunofluorescence (**H-J**). *** $P < 0.001$; ** $P < 0.01$; * $P < 0.05$.

Abbreviations: JQP, Jianpi Qingre Tongluo Prescription; LncHOTAIR, Lnc RNA HOTAIR; PC, OA-PBMCs (Osteoarthritis-Peripheral Blood Mononuclear Cells) +OA-CH (Osteoarthritis-chondrocytes); APN, Adiponectin; IL-1β/4/6/10, Interleukin-1β/4/6/10; ns, No statistical significance.

baicalein, quercetin, and kaempferol, may have a vital role in the treatment process. Baicalin is a kind of flavonoid isolated from the dried roots of Scutellaria Baicalensis Georgi, a dicotyledonous Lamiaceae, which is light yellow powders with bitter taste at room temperature. Baicalin has anti-inflammatory, cholesterol-lowering, antibacterial, anti-thrombosis, anti-allergy, diuretic, and spasmolytic effects. Former research reported[48,49] that baicalin protected against cartilage destruction, mitigated IL-1β-induced inflammation, and repressed IL-6 and TNF-α production in OA, underscoring baicalin as a promising agent for OA treatment. Quercetin is also a bioactive flavonoid that has shown significant joint protection against rheumatoid arthritis, gouty arthritis, and OA.[50] Samadi et al[51] reviewed many clinical trials of Quercetin for OA, showing that supplements containing Quercetin glycosides can improve OA related symptoms, and were included in the standard of treatment by the Japanese Orthopaedic Association in 2012.[52] In addition, mounting in vivo and in vitro experiments have found that quercetin and kaempferol not only down-regulates matrix degrading protease and inflammatory mediators in the OA-CH model but also promotes cartilage anabolic factor production and relieves cartilage degradation and inflammation in the OA rat model.[53–55]

Jian has found[56] that quercetin, kaempferol, and baicalein possesses essential biological effects and are enriched in many pathways including PI3K/AKT. In our study, JQP was featured by multi-pathways and multi-targets in OA treatment, and its core targets included AKT1. AKT1, a serine/threonine protein kinase, is extensively expressed in tissues and has a key role in PI3K/AKT pathway. Our KEGG results showed the enrichment of pathways including PI3K-AKT. Meanwhile, it was interesting to find that AKT1 was the common target of quercetin, kaempferol, and baicalein through the collection of target information of active ingredients, and the molecular docking results with puerarin and salvianolic acid B, the active ingredients of JQP identified by UPLC-MS/MS technique, showed low binding energy, the importance of the PI3K/AKT signaling pathway was confirmed.

Furthermore, studies[57,58] have shown that HOTAIR down-regulation conspicuously lowered PI3K and AKT phosphorylation. In a previous study, we identified characteristic lncRNA molecular markers of osteoarthritis through GEO database combined with machine learning strategies and verified them by experiment and obtained HOTAIR differentially expressed in OA patients.[59] Nonetheless, the function of HOTAIR in OA has not been studied in depth. Based on the prediction of data mining, network pharmacology and molecular docking, we conducted experimental verification in vitro. In order to simulate the disease state of OA patients, we innovatively built the co-culture model of PBMCs and CH for the first time, the concept of microenvironment has long been widely discussed in inflammatory tissues.[60,61] First, we detected the expression levels of HOTAIR, IL-1β, IL-6, IL-4, IL-10, and APN in co-cultured cells to comprehensively evaluate whether the co-cultured cells could meet the microenvironment requirements for simulating OA in vitro. In fact, our results once again confirm its reliability and feasibility. And here, we confirmed the high expression of HOTAIR in PC cells. Then through HOTAIR overexpression or small interference plasmid, APN overexpression plasmid and PI3K/AKT inhibitor, we found that high HOTAIR expression and phosphorylation of PI3K and AKT can reduce the cell viability of PC and induce the production of pro-inflammatory factors, while APN exists as a cartilage protective factor. In addition, through the observation of their interaction, we verified that the lncRNA HOTAIR/APN /PI3K/AKT axis plays an important role in the occurrence and development of OA. Drug-containing serum is collected from the serum of medically treated animals. It is a common method to study the molecular mechanism of the therapeutic effect of Chinese medicine.[62,63] In this study, the therapeutic effects of JQP against PC cells via the HOTAIR/APN/PI3K/AKT axis were investigated by cell experiments. The findings unraveled that JQP-containing serum was effective in facilitating CHs from OA patient, reducing inflammatory factor release, and augmenting APN levels, alleviating articular cartilage damage. Mechanistically, JQP-containing serum considerably diminished HOTAIR expression and phosphorylation of PI3K/AKT pathway, suppressed this pathway, and increased APN levels downstream of HOTAIR and upstream of PI3K/AKT pathway. Furthermore, JQP-containing serum lowered IL-6 and IL-1β levels and augmented IL-4 and IL-10 levels in the peripheral inflammatory matrix of cartilage cells, as well as preventing cartilage inflammatory damage in knee joints. This provides evidence for clinical use of JQP and the role of JQP in improving the pathology of OA cartilage inflammatory injury, and the next step will continue to design more detailed randomized controlled experiments and in vitro and in vivo experiments to explore its potential.

Conclusion

In general, the efficacy of JQP was confirmed via data mining. Then, the active targets of JQP were yielded with the use of network pharmacology and previous research, and the docking target was chosen based on degree value and the mechanism of JQP in OA treatment was further verified via in vitro experiments. JQP suppresses immune inflammation by down-regulating HOTAIR, thereby up-regulating APN, inhibiting PI3K/AKT pathway, and balancing inflammatory cytokines. In other words, JQP can treat OA by orchestrating HOTAIR/APN/PI3K/AKT and intervening in immune responses. These results highlight the role of JQP in improving immune inflammation and lipid metabolism and explain potential mechanisms for the treatment of OA (Supplementary Picture 2). The study has several advantages. We innovatively adopted a co-culture cell model to simulate the inflammatory microenvironment in OA patients, addressing the limitations of single-cell studies. In addition, gene co-editing techniques and network co-regulation analysis identified the mechanism targets. The combination of cell co-culture, gene co-editing and network co-regulation improved the rigor of the study design. However, there are some limitations to this study. First, it lacks animal experiments to observe the histopathological changes of OA. Second, the patients were selected from a single center. Future studies should increase our recruitment scope and expand the sample size to reduce data bias.

Abbreviations

ACR, American College of Rheumatology; AKT, Protein Kinase B; APN, Adiponectin; ARM, Association Rule Mining; BP, Biological Process; C3/4, Complement C3/4; CC, Cellular Components; CCK-8, Cell Counting Kit-8; CH, Chondrocytes; ELISA, Enzyme-linked immunosorbent assay; ESR, Erythrocyte Sedimentation Rate; GO, Gene Ontology; HQC, Huangqin Qingrechubi Capsule; hs-CRP, hs-C-Reactive Protein; IL-1β/4/6/10, Interleukin-1β/4/6/10; IF, Immunofluorescence; IgA/G/M, Immunoglobulin A/G/M; JQP, Jianpi Qingre Tongluo Prescription; LncRNA, Long noncoding RNA; OA, Osteoarthritis; OA-CH, Osteoarthritis-chondrocytes; PC, OA-PBMCs +OA-CH; KEGG, Kyoto Encyclopedia of Genes and Genomes; MF, Molecular Functions; NSAIDs, Non-steroidal anti-inflammatory drugs; PBMCs, Peripheral Blood Mononuclear Cell; PI3K, Phosphatidylinositol 3-kinase; PPI, Protein-Protein Interaction network; RT-qPCR, Real-time Fluorescence Quantitative PCR; SAS, Self Rating Anxiety Scale; SDS, Self Rating Depression Scale; si-RNA, Small interfering RNA; TC, Total cholesterol; TCMSP, Traditional Chinese Medicine Systems Pharmacology; TG, Triglyceride; TNF-α, Tumornecrosisfactor-α; VAS, The Visual Analogue Scale; WB, Western Blot; XFC, Xinfeng Capsule.

Data Sharing Statement

The data that support the findings of this study are available from the information Center of Anhui Hospital of Traditional Chinese Medicine obtains the electronic medical record information of effective OA inpatients from the SQL Server database, but restrictions apply to the availability of these data, which were used under license for the current study, and so are not publicly available. Data are, however, available from the authors upon reasonable request and with permission of the information Center.

Author Contributions

All authors made a significant contribution to the work reported, whether that is in the conception, study design, execution, acquisition of data, analysis and interpretation, or in all these areas; took part in drafting, revising or critically reviewing the article; gave final approval of the version to be published; have agreed on the journal to which the article has been submitted; and agree to be accountable for all aspects of the work.

Funding

This work was supported by Anhui Province 2023 natural science major project of colleges and universities (2023AH040112); the Key Projects of Scientific Research Projects of Higher Education Institutions in Anhui Province (Natural Sciences) (No. 2022AH050449); the University Synergy Innovation Program of Anhui Province (GXXT-2020-025); Anhui Provincial Laboratory of Applied Basis and Development of Internal Medicine of Modern Traditional

Chinese Medicine (2016080503B041); the Key Laboratory of Xin'an Ministry of Medical Education (No.2020xayx10), the 2021 open fund of Anhui Key Laboratory of applied basic and Development Research of modern internal medicine of traditional Chinese medicine (2021AKLMCM005), and the 2021 Anhui Province Major Difficult Diseases Collaborative Project of Traditional Chinese and Western Medicine (Anhui Traditional Chinese Medicine Development Secret [2021] No. 70).

Disclosure

The authors declare no conflicts of interest in this work.

References

1. Dell'Isola A, Recenti F, Englund M, Kiadaliri A. Twenty-year trajectories of morbidity in individuals with and without osteoarthritis. *RMD Open*. 2024;10(2). doi:10.1136/rmdopen-2024-004164
2. Belluzzi E, Olivotto E, Toso G, et al. Conditioned media from human osteoarthritic synovium induces inflammation in a synoviocyte cell line. *Connect Tissue Res*. 2019;60(2):136–145. doi:10.1080/03008207.2018.1470167
3. Motta F, Barone E, Sica A, Selmi C. Inflammaging and Osteoarthritis. *Clin Rev Allerg Immu*. 2023;64(2):222–238. doi:10.1007/s12016-022-08941-1
4. Emmi A, Stocco E, Boscolo-Berto R, et al. Infrapatellar fat pad-synovial membrane anatomo-functional unit: microscopic basis for Piezo1/2 mechanosensors involvement in osteoarthritis pain. *Front Cell Dev Biol*. 2022;10:886604. doi:10.3389/fcell.2022.886604
5. Jenei-Lanzl Z, Meurer A, Zaucke F. Interleukin-1β signaling in osteoarthritis - chondrocytes in focus. *Cell Signal*. 2019;53:212–223. doi:10.1016/j.cellsig.2018.10.005
6. Ohtsuki T, Hatipoglu OF, Asano K, Inagaki J, Nishida K, Hirohata S. Induction of CEMIP in chondrocytes by inflammatory cytokines: underlying mechanisms and potential involvement in osteoarthritis. *Int J Mol Sci*. 2020;21(9):3140. doi:10.3390/ijms21093140
7. Zhang K, Ji Y, Dai H, et al. High-density lipoprotein cholesterol and apolipoprotein a1 in synovial fluid: potential predictors of disease severity of primary knee osteoarthritis. *Cartilage*. 2021;13(1_suppl):1465s–1473s. doi:10.1177/19476035211007919
8. Pięta A, Frączek B, Wiecek M, Mazur-Kurach P. Impact of paleo diet on body composition, carbohydrate and fat metabolism of professional handball players. *Nutrients*. 2023;15(19):4155. doi:10.3390/nu15194155
9. Asbaghi O, Kelishadi MR, Larky DA, et al. The effects of green tea extract supplementation on body composition, obesity-related hormones and oxidative stress markers: a grade-assessed systematic review and dose-response meta-analysis of randomised controlled trials. *Br J Nutr*. 2024;131(7):1125–1157. doi:10.1017/S000711452300260X
10. Verhoeven BM, Mei S, Olsen TK, et al. The immune cell atlas of human neuroblastoma. *Cell Rep Med*. 2022;3(6):100657. doi:10.1016/j.xcrm.2022.100657
11. Chen H, Li P, Chen J, et al. Peripheral blood mononuclear cell microRNAs are novel biomarkers for diagnosing and monitoring Crohn's disease. *FASEB J*. 2022;36(10):e22549. doi:10.1096/fj.202200452R
12. Alsalameh RJ, Casey RC, Mollenhauer J, Kalden JR, Burmester GR, Alsalameh SM. Induction of proliferation and pro-inflammatory cytokine production in rheumatoid arthritis peripheral blood mononuclear cells by a 65 KDa chondrocyte membrane-specific, constitutive target autoantigen (CH65). *Int j Rheum Dis*. 2017;20(9):1132–1141. doi:10.1111/1756-185X.12167
13. Platzer H, Nees TA, Reiner T, et al. Impact of mononuclear cell infiltration on chondrodestructive MMP/ADAMTS production in osteoarthritic knee joints-an ex vivo study. *J Clin Med*. 2020;9(5):1279. doi:10.3390/jcm9051279
14. Moradi N, Fadaei R, Ahmadi R, Kazemian E, Fallah S. Lower expression of miR-10a in coronary artery disease and its association with pro/anti-inflammatory cytokines. *Clin Lab*. 2018;64(5):847–854. doi:10.7754/Clin.Lab.2018.171222
15. Ramos-Ramírez P, Malmhäll C, Tliba O, Rådinger M, Bossios A. Adiponectin/AdipoR1 axis promotes IL-10 release by human regulatory T cells. *Front Immunol*. 2021;12:677550.
16. Bannuru RR, Osani MC, Vaysbrot EE, et al. OARSI guidelines for the non-surgical management of knee, Hip, and polyarticular osteoarthritis. *Osteoarthr Cartilage*. 2019;27(11):1578–1589. doi:10.1016/j.joca.2019.06.011
17. Ahmad SS, Gantenbein B, Evangelopoulos DS, et al. Arthroplasty - current strategies for the management of knee osteoarthritis. *Swiss Med Wkly*. 2015;145:w14096. doi:10.4414/smw.2015.14096
18. Grigore A, Vulturescu V. Natural Approach in Osteoarthritis Therapy. *Recent Adv Inflamm Allergy Drug Discov*. 2022;16(1):26–31. doi:10.2174/2772270816666220331163707
19. He Q, Yang J, Pan Z, et al. Biochanin A protects against iron overload associated knee osteoarthritis via regulating iron levels and NRF2/System xc-/GPX4 axis. *Biomed Pharmacother*. 2023;157:113915. doi:10.1016/j.biopha.2022.113915
20. Tu J, Huang W, Zhang W, Mei J, Zhu C. The emerging role of lncRNAs in chondrocytes from osteoarthritis patients. *Biomed Pharmacother*. 2020;131:110642. doi:10.1016/j.biopha.2020.110642
21. Xin X, Li Q, Fang J, Zhao T. LncRNA HOTAIR: a Potential Prognostic Factor and Therapeutic Target in Human Cancers. *Front Oncol*. 2021;11:679244. doi:10.3389/fonc.2021.679244
22. Rajagopal T, Talluri S, Akshaya RL, Dunna NR. HOTAIR LncRNA: a novel oncogenic propellant in human cancer. *Clin Chim Acta*. 2020;503:1–18. doi:10.1016/j.cca.2019.12.028
23. Price RL, Bhan A, Mandal SS. HOTAIR beyond repression: in protein degradation, inflammation, DNA damage response, and cell signaling. *DNA Repair*. 2021;105:103141. doi:10.1016/j.dnarep.2021.103141
24. Wang B, Sun Y, Liu N, Liu H. LncRNA HOTAIR modulates chondrocyte apoptosis and inflammation in osteoarthritis via regulating miR-1277-5p/SGTB axis. *Wound Repair Regen*. 2021;29(3):495–504. doi:10.1111/wrr.12908
25. Liang Q, Asila A, Deng Y, Liao J, Liu Z, Fang R. Osteopontin-induced lncRNA HOTAIR expression is involved in osteoarthritis by regulating cell proliferation. *BMC Geriatr*. 2021;21(1):57. doi:10.1186/s12877-020-01993-y

26. Liu J, Jia S, Yang Y, et al. Exercise induced meteorin-like protects chondrocytes against inflammation and pyroptosis in osteoarthritis by inhibiting PI3K/Akt/NF-κB and NLRP3/caspase-1/GSDMD signaling. *Biomed Pharmacother*. 2023;158:114118. doi:10.1016/j.biopha.2022.114118
27. Chen L, Liu P, Feng X, Ma C. Salidroside suppressing LPS-induced myocardial injury by inhibiting ROS-mediated PI3K/Akt/mTOR pathway in vitro and in vivo. *J Cell Mol Med*. 2017;21(12):3178–3189. doi:10.1111/jcmm.12871
28. Chen X, Liu J, Sun Y, et al. Correlation analysis of differentially expressed long non-coding RNA HOTAIR with PTEN/PI3K/AKT pathway and inflammation in patients with osteoarthritis and the effect of baicalin intervention. *J Orthop Surg Res*. 2023;18(1):34. doi:10.1186/s13018-023-03505-1
29. Wang F, Meng M, Chen L, Wang XY, Sun Q. Development and validation of a high-performance thin-layer chromatographic fingerprint method for the evaluation of QiYi capsules with the reference of myotonin. *JPC J Planar Chromatogr Mod TLC*. 2014;27(3):199–203. doi:10.1556/JPC.27.2014.3.9
30. Zhou Q, Liu J, Xin L, et al. Exploratory compatibility regularity of Traditional Chinese Medicine on osteoarthritis treatment: a data mining and random walk-based identification. *Evid Based Complement Altern Med*. 2021;2021:2361512. doi:10.1155/2021/2361512
31. Hu Y, Liu J, Qi Y, et al. Integrating clinical data mining, network analysis and experimental validation reveal the anti-inflammatory mechanism of Huangqin Qingre Chubi Capsule in rheumatoid arthritis treatment. *J Ethnopharmacol*. 2024;329:118077. doi:10.1016/j.jep.2024.118077
32. Fang Y, Liu J, Xin L, et al. Xinfeng capsule inhibits lncRNA NONHSAT227927.1/TRAF2 to alleviate NF-κB-p65-induced immuno-inflammation in ankylosing spondylitis. *J Ethnopharmacol*. 2024;323:117677. doi:10.1016/j.jep.2023.117677
33. Liu R, Liu JQ, Liu XC. Study on the extraction technology of Jianpi Hua Wet Qingre Tongluo recipe. *Shi Zhen Guo Yi Guo Yao*. 2022;33(10):2401–2403.
34. Dong XT, Ke JT, Gan P, et al. To explore the quality markers of Huangqin Qingre Chubi Capsule in the treatment of rheumatoid arthritis based on network pharmacology combined with pharmacokinetics and target verification. *Acta Pharm Sin*. 2023;58:1422–1429.
35. Wang P, Li L, Yang H, et al. Chromatographic fingerprinting and quantitative analysis for the quality evaluation of Xinkeshu tablet. *J Pharm Anal*. 2012;2(6):422–430. doi:10.1016/j.jpha.2012.05.006
36. Zhou Q, Liu J, Zhu Y. [Based on AMPK/Foxo3a axis, the mechanism of strengthening spleen for dampness and clearing heat for colligation in improving oxidative stress in rats with adjuvant arthritis was studied] 基于AMPK/Foxo3a轴研究健脾化湿、清热通络法改善佐剂性关节炎大鼠氧化应激状态的机制. *Feng Shi Bing Yu Guan Jie Yan*. 2019;9(08):1–6+17. Chinese.
37. Wang J, Liu J, Wen JT, Wang X. Retrospective data mining study on circRNA0003353, immune inflammation and bone metabolism indexes of patients with damp-heat obstruction syndrome of RA by strengthening spleen and clearing heat Tongluo. *Zhong Yi Yao Lin Chuang*. 2022;4:725–730.
38. Liu J, Wang Y, Sun Y, et al. "Efficacy and safety of Xinfeng capsule in the treatment of osteoarthritis: a multicenter, randomized, double-blinded, controlled trial". *J Tradit Chin Med*. 2020;40(2):284–295.
39. Kolasinski SL, Neogi T, Hochberg MC, et al. 2019 American College of Rheumatology/Arthritis Foundation Guideline for the management of osteoarthritis of the hand, hip, and knee. *Arthritis Rheumatol*. 2020;72(2):220–233. doi:10.1002/art.41142
40. Shrestha B, Dunn L. The declaration of Helsinki on medical research involving human subjects: a review of seventh revision. *J Nepal Health Res Counc*. 2020;17(4):548–552. doi:10.33314/jnhrc.v17i4.1042
41. Hu Y, Liu J, Xin L, et al. Huangqin Qingre Chubi Capsule is associated with reduced risk of readmission in patients with rheumatoid arthritis: a real-world retrospective cohort study. *Int J Gen Med*. 2023;16:4819–4834. doi:10.2147/IJGM.S431124
42. Ding L, Xie S, Zhang S, et al. Delayed Comparison and Apriori Algorithm (DCAA): a tool for discovering protein-protein interactions from time-series phosphoproteomic data. *Front Mol Biosci*. 2020;7:606570. doi:10.3389/fmolb.2020.606570
43. Fang Y, Liu J, Xin L, et al. Identifying compound effect of drugs on rheumatoid arthritis treatment based on the association rule and a random walking-based model. *Biomed Res Int*. 2020;2020:4031015. doi:10.1155/2020/4031015
44. Wang X, Chang J, Zhou G, et al. The Traditional Chinese Medicine Compound Huangqin Qingre Chubi Capsule Inhibits the pathogenesis of rheumatoid arthritis through the CUL4B/Wnt pathway. *Front Pharmacol*. 2021;12:750233. doi:10.3389/fphar.2021.750233
45. Liu X, Wang Y, Zhang Y, Jiang H, Huo X, Liu R. Integrated bioinformatic analysis and experimental validation to reveal the mechanisms of Xinfeng Capsule against rheumatoid arthritis. *Comb Chem High Throughput Scr*. 2023;26(12):2161–2169.
46. Wang Y, Liu J, Wang Y, Sun Y. Effect of Xinfeng capsule in the treatment of active rheumatoid arthritis: a randomized controlled trial. *J Tradit Chin Med*. 2015;35(6):626–631. doi:10.1016/S0254-6272(15)30150-3
47. Chen M, Sun Q. Systemic pharmacology understanding of the key mechanism of Sedum sarmentosum Bunge in treating hepatitis. *N-s Arch Pharmacol*. 2021;394(2):421–430. doi:10.1007/s00210-020-01952-9
48. Yang X, Zhang Q, Gao Z, Yu C, Zhang L. Baicalin alleviates IL-1β-induced inflammatory injury via down-regulating miR-126 in chondrocytes. *Biomed Pharmacother*. 2018;99:184–190. doi:10.1016/j.biopha.2018.01.041
49. Chen C, Zhang C, Cai L, et al. Baicalin suppresses IL-1β-induced expression of inflammatory cytokines via blocking NF-κB in human osteoarthritis chondrocytes and shows protective effect in mice osteoarthritis models. *Int Immunopharmacol*. 2017;52:218–226. doi:10.1016/j.intimp.2017.09.017
50. Goyal A, Agrawal N. Quercetin: a potential candidate for the treatment of arthritis. *Curr Mol Med*. 2022;22(4):325–335.
51. Samadi F, Kahrizi MS, Heydari F, et al. Quercetin and osteoarthritis: a mechanistic review on the present documents. *Pharmacology*. 2022;107(9–10):464–471. doi:10.1159/000525494
52. Kanzaki N, Saito K, Maeda A, et al. Effect of a dietary supplement containing glucosamine hydrochloride, chondroitin sulfate and quercetin glycosides on symptomatic knee osteoarthritis: a randomized, double-blind, placebo-controlled study. *J Sci Food Agr*. 2012;92(4):862–869. doi:10.1002/jsfa.4660
53. Aleebrahim-Dehkordi E, Soveyzi F, Arian AS, Hamedanchi NF, Hasanpour-Dehkordi A, Rafieian-Kopaei M. Quercetin and its role in reducing the expression of pro-inflammatory cytokines in osteoarthritis. *Antiinflamm Antiallergy Agents Med Chem*. 2023;21(3):153–165. doi:10.2174/1871523022666221213155905
54. Xiao Y, Liu L, Zheng Y, Liu W, Xu Y. Kaempferol attenuates the effects of XIST/miR-130a/STAT3 on inflammation and extracellular matrix degradation in osteoarthritis. *Future Med Chem*. 2021;13(17):1451–1464. doi:10.4155/fmc-2021-0127

55. Hu Y, Gui Z, Zhou Y, Xia L, Lin K, Xu Y. Quercetin alleviates rat osteoarthritis by inhibiting inflammation and apoptosis of chondrocytes, modulating synovial macrophages polarization to M2 macrophages. *Free Radical Bio Med*. 2019;145:146–160. doi:10.1016/j.freeradbiomed.2019.09.024
56. Jian GH, Su BZ, Zhou WJ, Xiong H. Application of network pharmacology and molecular docking to elucidate the potential mechanism of Eucommia ulmoides-Radix Achyranthis Bidentatae against osteoarthritis. *BioData Min*. 2020;13(1):12. doi:10.1186/s13040-020-00221-y
57. Liu F, Wang Y, Huang D, Sun Y. LncRNA HOTAIR regulates the PI3K/AKT pathway via the miR-126-3p/PIK3R2 axis to participate in synovial angiogenesis in rheumatoid arthritis. *Immun Inflamm Dis*. 2023;11(10):e1064. doi:10.1002/iid3.1064
58. Li Z, Qian J, Li J, Zhu C. Knockdown of lncRNA-HOTAIR downregulates the drug-resistance of breast cancer cells to doxorubicin via the PI3K/AKT/mTOR signaling pathway. *Exp ther med*. 2019;18(1):435–442. doi:10.3892/etm.2019.7629
59. Zhou Q, Liu J, Xin L, Fang Y, Qi Y, Hu Y. [Identification of characteristic lncRNA molecular markers in osteoarthritis by integrating GEO database and machine learning strategies and experimental validation] GEO数据库联合机器学习策略识别骨关节炎特征性lncRNA分子标志物及实验验证. *Sichuan Da Xue Xue Bao Yi Xue Ban*. 2023;54(5):899–907. Chinese. doi:10.12182/20230960101
60. Guo J, Wang F, Hu Y, et al. Exosome-based bone-targeting drug delivery alleviates impaired osteoblastic bone formation and bone loss in inflammatory bowel diseases. *Cell Rep Med*. 2023;4(1):100881. doi:10.1016/j.xcrm.2022.100881
61. Korsten S, Vromans H, Garssen J, Willemsen LEM. Butyrate protects barrier integrity and suppresses immune activation in a Caco-2/PBMC Co-culture model while HDAC inhibition mimics butyrate in restoring cytokine-induced barrier disruption. *Nutrients*. 2023;15(12):2760. doi:10.3390/nu15122760
62. Tang Z, Li W, Xie H, Jiang S, Pu Y, Xiong H. Taohong Siwu-containing serum enhances angiogenesis in rat aortic endothelial cells by regulating the VHL/HIF-1α/VEGF signaling pathway. *Evid Based Complement Altern Med*. 2021;2021:6610116. doi:10.1155/2021/6610116
63. Yin J, Luo Y, Deng H, et al. Hugan Qingzhi medication ameliorates hepatic steatosis by activating AMPK and PPARα pathways in L02 cells and HepG2 cells. *J Ethnopharmacol*. 2014;154(1):229–239. doi:10.1016/j.jep.2014.04.011